

School of Electrical Engineering and Computing
Department of Electrical and Computer Engineering

Improving the Performance of MIMO Relay Networks
Using Parallel Relays

Apriana Toding

This thesis is presented for the degree of
Doctor of Philosophy
of
Curtin University

February 2014

Declaration

To the best of my knowledge and belief this thesis contains no material previously published by any other person except where due acknowledgment has been made.

This thesis contains no material which has been accepted for the award of any other degree or diploma in any university.

Signature:

Date:

To

*my parents, my husband Lujiber, and my kids Aurilia and
Edward*

Acknowledgements

First of all, I would like to thank my thesis supervisor Associate Professor Yue Rong for his constant support and encouragement during my Ph.D. studies. His invaluable guidance and timely correspondence directed me to reach the goal. He was consistently patient and caring in his instructive and research support, which guided me to pursue the right path.

I also thank all members of my thesis committee for helping me to complete the thesis. The appreciated comments and recommendations from Dr. Roy Howard, Chairperson of my thesis committee, Dr. King-Sun Chan, Associate supervisor of my thesis, and Prof. Sven Nordholm, Head of the Department, especially during the group seminars, helped me to improve a lot.

I thank my friend Dr. Muhammad R. A. Khandaker for fruitful assistance which led to several interesting results obtained during my Ph.D. studies. Also thank my research peers at the Communication Technology and Signal Processing (CSP) group of the Department for the good times and the kindly help they gave me during my time here.

I am thankful to UKI-Paulus, DIKTI, Pemprov Sulawesi Selatan, and Pemda Toraja Utara, Indonesia for the financial support they have provided me during the course of my Ph.D. studies. I am also grateful to all administrative staffs at Faculty of Science and Engineering, and Student Central of Curtin University for the administrative support they have given me during the course of my Ph.D. studies.

Most of all, I am grateful to my parents, my husband Lujiber, and my kids Aurilia and Edward for their patience, wonderful love, and moral support to me. I would like to finish off by thanking my Creator for making my life beautiful.

Abstract

Recently, multiple-input multiple-output (MIMO) relay communication systems have attracted much research interest, and provided significant improvement in terms of both spectral efficiency and link reliability. This thesis aims at improving the performance of MIMO relay communication systems using parallel relays and successive interference cancellation (SIC) technique.

In the first part of the thesis, we propose the optimal transmit beamforming vector and the relay amplifying factors for a MIMO relay communication system with distributed single-antenna relay nodes when a single data stream is transmitted from the source to destination. The proposed joint source and relay beamforming algorithm provides an improved bit-error-rate (BER) performance.

The second part of the thesis focuses on parallel MIMO relay communication systems where each relay has multiple antennas and multiple data streams are transmitted from the source to the destination. We derive the optimal structure of relay amplifying matrices when a linear minimal mean-squared error (MSE) receiver is used at the destination node and each relay node is subject to power constraint. Simulation results demonstrate the effectiveness of the proposed source and relay matrices design which minimizes the MSE of the signal waveform estimation using the projected gradient (PG) approach.

To reduce the complexity of the algorithm in the second part of the thesis, we propose a simplified source and relay matrices design by first relaxing the power constraint at each relay node to the power constraint at the output of the second-hop channel. After solving the relaxed optimisation problem, the relay matrices are then scaled to satisfy the individual power constraint at each relay node. Simulation results show a good performance-complexity tradeoff of the simplified algorithm.

In the fourth part of the thesis, we investigate the optimal structure of the source precoding matrix and the relay amplifying matrices for MIMO relay communication systems with parallel relay nodes when a nonlinear MMSE-DFE receiver is used at the destination node. The MMSE criterion is used to detect the transmitted signal at each stream. We show that the optimal source precoding matrix and the optimal relay amplifying matrices have a beamforming structure. By using a DFE receiver, we can remove the effect of interferences of data stream we have already recovered from the subsequent streams. Therefore, introducing a nonlinear MMSE-DFE receiver at the destination node yields further improvement in the system BER performance compared with the parallel MIMO relay communication systems using a linear MMSE receiver.

Author's Note

Parts of this thesis and concepts from it have been previously published in the following journal and/or conference papers.

Journal Papers

- [1] A. Toding, M. R. A. Khandaker, and Y. Rong, "Joint Source and Relay Optimization for Parallel MIMO Relay Networks", *EURASIP Journal on Advances in Signal Processing*, 2012:174.
- [2] A. Toding, M. R. A. Khandaker, and Y. Rong, "Joint Source and Relay Design for MIMO Multi-Relay Systems Using Projected Gradient Approach", *EURASIP Journal on Wireless Commun. Network.*, submitted, Aug. 2013.

Conference Papers

- [1] A. Toding, M. R. A. Khandaker, and Y. Rong, "Optimal Joint Source and Relay Beamforming for Parallel MIMO Relay Networks", in *Proc. 6th Int. Conf. Wireless Commun., Networking and Mobile Computing (WiCOM'2010)*, Chengdu, China, Sep. 23-25, 2010.
- [2] A. Toding, M. R. A. Khandaker, and Y. Rong, "Joint Source and Relay Optimization for Parallel MIMO Relays Using MMSE-DFE Receiver", in *Proc. 16th Asia-Pacific Conference on Communications (APCC'2010)*, Auckland, New Zealand, Nov. 1-3, 2010, pp. 12-16.
- [3] A. Toding, M. R. A. Khandaker, and Y. Rong, "Joint Source and Relay Optimization for Distributed MIMO Relay System", in *Proc. 17th Asia-Pacific Conference on Communications (APCC'2011)*, Sabah, Malaysia, Oct. 2-5, 2011, pp. 604-608.
- [4] A. Toding and Y. Rong, "Investigating Successive Interference Cancellation in MIMO Relay Network", in *Proc. IEEE TENCON*, Bali, Indonesia, Nov. 21-24, 2011, pp. 359-363.

Contents

| | |
|--|-------------|
| List of Figures | xiii |
| List of Tables | xv |
| List of Acronyms | xvii |
| 1 Introduction | 1 |
| 1.1 Background | 1 |
| 1.2 Notations | 3 |
| 1.3 Receiver Algorithms for MIMO Systems | 4 |
| 1.4 Thesis Overview and Contributions | 7 |
| 2 MIMO Transceiver Design with Distributed Relay Nodes | 11 |
| 2.1 Overview of Single-Antenna Relay Technique | 11 |
| 2.2 Distributed MIMO Relay System Model | 12 |
| 2.3 Optimal Source and Relay Design | 14 |
| 2.3.1 Optimal Relay Factors | 16 |
| 2.3.2 Joint Source and Relay Optimization Algorithm | 17 |
| 2.4 Numerical Examples | 20 |
| 2.5 Chapter Summary | 22 |
| 3 Parallel MIMO Relay Design Based on Linear Receiver | 23 |
| 3.1 Existing Works with Linear MMSE Receiver | 23 |
| 3.2 Parallel MIMO Relay System | 24 |
| 3.3 Joint Source and Relay Matrices Optimization | 27 |
| 3.3.1 Optimal Structure of Relay Amplifying Matrices | 28 |

| | | |
|----------|--|-----------|
| 3.3.2 | Optimal Source Precoding Matrix | 30 |
| 3.4 | Numerical Examples | 31 |
| 3.5 | Chapter Summary | 34 |
| 3.A | Proof of Theorem 3.1. | 35 |
| 3.B | Proof of Theorem 3.2. | 35 |
| 4 | Simplified Source and Relay Matrices Design | 37 |
| 4.1 | MMSE Relay Design Algorithm | 37 |
| 4.2 | Numerical Examples | 41 |
| 4.3 | Chapter Summary | 43 |
| 5 | Parallel MIMO Relay Design Based on Nonlinear Receiver | 45 |
| 5.1 | Overview of Known Techniques | 45 |
| 5.2 | Performance Comparison of Linear and Nonlinear Receivers | 46 |
| 5.3 | Optimal Source and Relay Design with DFE | 47 |
| 5.4 | Numerical Examples | 53 |
| 5.5 | Chapter Summary | 54 |
| 6 | Conclusions and Future Work | 57 |
| 6.1 | Concluding Remarks | 57 |
| 6.2 | Future Works | 58 |
| | Bibliography | 59 |

List of Figures

| | | |
|-----|---|----|
| 1.1 | Block diagram of a parallel MIMO relay communication system using SIC technique. | 3 |
| 1.2 | Block diagram of the equivalent MIMO channel. | 4 |
| 1.3 | Successive interference cancellation technique. | 6 |
| 2.1 | Block diagram of a parallel MIMO relay communication system with a single data stream. | 13 |
| 2.2 | Block diagram of the equivalent MIMO relay system with a single data stream. | 14 |
| 2.3 | Example 2.1 BER versus SNR_s with varying K . $N_s = N_d = 3$, $\text{SNR}_r = 20\text{dB}$ | 20 |
| 2.4 | Example 2.2 BER versus SNR_s with varying K . $N_s = N_d = 5$, $\text{SNR}_r = 20\text{dB}$ | 21 |
| 2.5 | Example 2.1 BER versus SNR_r with varying K . $N_s = N_d = 3$, $\text{SNR}_s = 20\text{dB}$ | 21 |
| 3.1 | Block diagram of a parallel MIMO relay communication system with multiple data streams. | 25 |
| 3.2 | Block diagram of the equivalent MIMO relay system with multiple data streams. | 26 |
| 3.3 | Example 3.1 Normalized MSE versus SNR_s with $K = 3$ | 32 |
| 3.4 | Example 3.1 Normalized MSE versus SNR_r with $K = 3$ | 32 |
| 3.5 | Example 3.2 BER versus SNR_s with $K = 3$ | 33 |
| 3.6 | Example 3.3 BER versus SNR_s with different K | 34 |
| 4.1 | Block diagram of the equivalent MIMO relay system with multiple data streams. | 38 |

| | | |
|-----|---|----|
| 4.2 | Example 4.1 BER versus SNR_s with $K = 3$ | 42 |
| 4.3 | Example 4.2 BER versus SNR_s with varying K | 43 |
| 5.1 | BER versus SNR_s . $N_s = N_r = N_d = 2$, $K = 1$ and $\text{SNR}_r = 20\text{dB}$ for MIMO relay channel. | 47 |
| 5.2 | BER versus SNR_r . $N_s = N_r = N_d = 2$, $K = 1$ and $\text{SNR}_s = 20\text{dB}$ for MIMO relay channel. | 48 |
| 5.3 | Block diagram of the equivalent MIMO relay system with SIC technique. | 48 |
| 5.4 | Example 5.1 BER versus SNR_s with $K = 3$ | 53 |
| 5.5 | Example 5.2 BER versus SNR_s with varying K | 54 |

List of Tables

| | | |
|-----|---|----|
| 2.1 | Procedure of solving the problem (2.13)-(2.15) by the proposed iterative algorithm. | 19 |
| 2.2 | Iterations required till convergence in the proposed algorithm | 22 |
| 3.1 | Procedure of applying the projected gradient algorithm to solve the problem (3.17)-(3.18) | 30 |
| 3.2 | Procedure of solving the problem (3.10)-(3.12). | 31 |

List of Acronyms

| | |
|-----------------|--|
| AF | amplify and forward |
| BER | bit-error-rate |
| BPSK | binary phase shift keying |
| BS | base station |
| CF | compress and forward |
| CSI | channel state information |
| DF | decode and forward |
| DFE | decision feedback equalizer |
| EVD | eigenvalue decomposition |
| i.i.d. | independent and identically distributed |
| JSR-PG | joint source and relay optimization algorithm using the projected gradient |
| LMMSE | linear minimum mean-squared error |
| MIMO | multiple-input multiple-output |
| MMSE | minimum mean-squared error |
| MMSE-DFE | minimum mean-squared error-decision feedback equalizer |
| MSE | mean-squared error |
| NAF | naive amplify-and-forward |

| | |
|---------------|---|
| ORO | optimal relay only |
| ORO-PG | optimal relay-only algorithm using the projected gradient |
| PG | projected gradient |
| PSD | positive semi-definite |
| SDP | semi-definite programming |
| SIC | successive interference cancellation |
| SISO | single-input single-output |
| SNR | signal-to-noise ratio |
| SVD | singular value decomposition |
| ZF | zero-forcing |

Chapter 1

Introduction

This thesis aims at developing and studying advanced algorithms for multiple-input multiple-output (MIMO) relay communication systems using parallel relays and successive interference cancellation (SIC) technique. In this introductory chapter, we briefly present necessary background on MIMO relay communication systems using parallel relays and SIC technique and overview the contributions of the thesis.

1.1 Background

In order to establish a reliable wireless transmission, one needs to compensate for the effects of signal fading due to multi-path propagation and strong shadowing. One way to address these issues is to transmit the signal through one or more relays [1–23], which can be accomplished via a wireless network consisting of geographically separated nodes. And then the basic motivation behind the use of cooperative communications lies in the exploitation of spatial diversity provided by the network nodes [9, 14–18], as well as the efficient use of power resources [19, 20, 24–29] which can be achieved by a scheme that simply receives and forwards a given information, yet designed under certain optimality criterion.

Wireless relaying systems have lots of advantages over traditional direct transmission systems and have drawn considerable interest from both the academic and industrial communities [30–34]. Relays can help improve the system capacity by decreasing the per-hop transmitter-receiver distance, decrease the infrastructure cost since they are much cheaper than base station (BS), and extend the network coverage [9, 13, 14, 35–39].

A three-terminal relay channel model was first studied in the 1970's as in [1, 2]. Relay schemes can be broadly categorized into three general groups: amplify-and-forward (AF), decode-and-forward (DF), and compress-and-forward (CF). In the AF scheme, the relay nodes amplify the received signal and rebroadcast the amplified signals toward the destination node [6, 21, 37, 40–47]. In the DF scheme, the relay nodes first decode the received signals and then forward the re-encoded signals toward the destination node [5, 22, 32, 48–50]. In the CF method, the relay nodes compress the received signals by exploiting the statistical dependencies between the signals at the nodes [32, 51–53].

When nodes in the relay system are installed with multiple antennas, we call such relay system MIMO relay communication system. Recently, MIMO relay communication systems have attracted much research interest and provided significant improvement in terms of both spectral efficiency and link reliability [7, 12, 37, 38, 41, 54–72]. In the meantime, work is being carried out on the factors affecting MIMO relay channels. Some proposed designs of the transmitter, receiver, and relay matrices show that increasing the number of relay antennas can reduce the system cost of building BS, increase the reliability of signals that arrive at the receiver, increase the channel capacity, improve the coverage area and increase the system diversity.

The main issue in a MIMO relay wireless communication system is to build the communication when there are some obstacles between transmitter and receiver. An efficient way to combat the problem is to use multiple parallel relays between the transmitter and the receiver which can provide more diversity and larger coverage area and overcome any possible shadowing effect [73–75].

Two types of receiver architectures are considered at the destination node, namely the linear receiver and the nonlinear receiver. For complexity reduction reasons, there has been great interest in the class of linear receivers such as zero-forcing (ZF) and minimum mean-squared error (MMSE) receivers [24, 27, 57, 58, 68, 76–86]. The ZF receiver first inverts the channel matrix so that each data stream can be recovered via a single-input single-output (SISO) decoding algorithm. The MMSE receiver does the same except with a regularized channel inverse that accounts for possible noise amplification. It has been shown in many recent works [26, 49, 87–104] that nonlinear receivers yield better performance compared to linear receivers at the cost of increased computational complexity. Even the simplified nonlinear receivers such as the decision feedback equalizer (DFE) based on the MMSE/ZF criterion can achieve performance gain. Both the MMSE and ZF schemes permit the use of powerful channel codes that

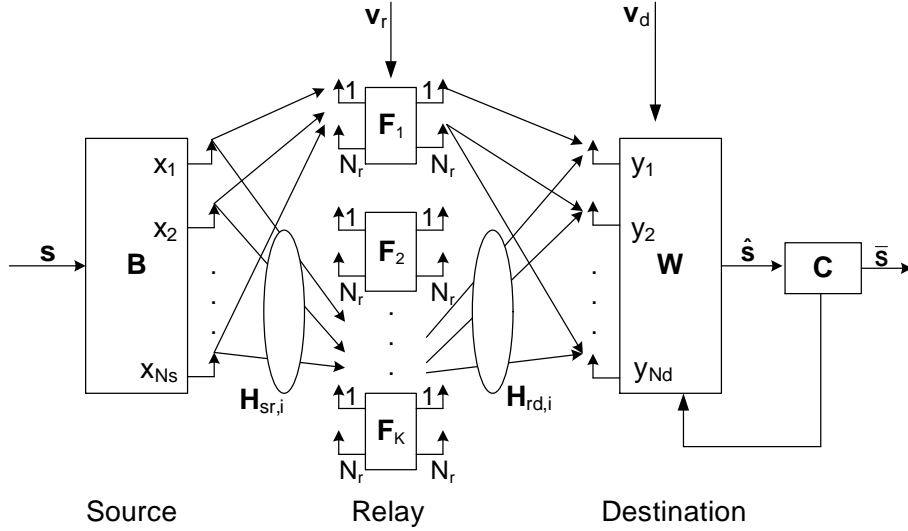


Figure 1.1: Block diagram of a parallel MIMO relay communication system using SIC technique.

can achieve high data rates at practically-relevant signal-to-noise ratio (SNR). The DFE technique is also well-known as the SIC technique. A nonlinear DFE receiver recovers the source signals successively by exploiting the finite alphabet property of the source signals. By using a DFE receiver we can remove the effect of interferences of the data streams we have already recovered from the subsequent streams. In this thesis, both linear and nonlinear methods have been proposed in parallel MIMO relay communication systems to separate the spatially multiplexed inputs at the receiver. A typical MIMO relay communication system with the DFE receiver is illustrated in Fig. 1.1, where \mathbf{s} is an $N_b \times 1$ source symbol vector, \mathbf{B} is an $N_s \times N_b$ source precoding matrix, $\mathbf{F}_1, \dots, \mathbf{F}_K$ are $N_r \times N_r$ amplifying matrices at the relay nodes, \mathbf{W} is an $N_d \times N_b$ receive weight matrix, \mathbf{C} is an $N_b \times N_b$ strictly upper-triangle feedback matrix of the DFE receiver, and $\bar{\mathbf{s}}$ is the estimated signal waveform vector. This thesis aims at optimizing \mathbf{B} , $\mathbf{F}_1, \dots, \mathbf{F}_K$, \mathbf{W} , and \mathbf{C} to minimize the MSE of the signal waveform estimation at the destination node.

1.2 Notations

The notations used in this thesis are as follows: Lower case letters are used to denote scalars, e.g. s, n . Bold face lower case letters denote vectors, e.g. \mathbf{s}, \mathbf{n} . Bold face upper

case letters are reserved for matrices, e.g. \mathbf{S} , \mathbf{N} . For matrices, $(\cdot)^T, (\cdot)^*, (\cdot)^H, (\cdot)^{-1}$, and $(\cdot)^+$ denote transpose, complex conjugate, Hermitian transpose, inversion, and pseudo-inverse operations, respectively. $\text{rank}(\cdot)$ and $\text{tr}(\cdot)$ denote the rank and trace of matrices, respectively. $\text{diag}(\mathbf{a})$ stands for a diagonal matrix with the vector \mathbf{a} as the main diagonal and zero elsewhere. $\mathbb{E}[\cdot]$ represents the statistical expectation, $\text{bd}[\cdot]$ stands for a block-diagonal matrix, and $\|\cdot\|$ denotes the maximum among the absolute value of all elements in the matrix. An N dimensional identity matrix is denoted as \mathbf{I}_N , $(\cdot)^n$ denotes the variable at the n th iteration, and $[x]^\dagger \triangleq \max(x, 0)$. Note that the scope of any variable in each chapter is limited to that particular chapter.

1.3 Receiver Algorithms for MIMO Systems

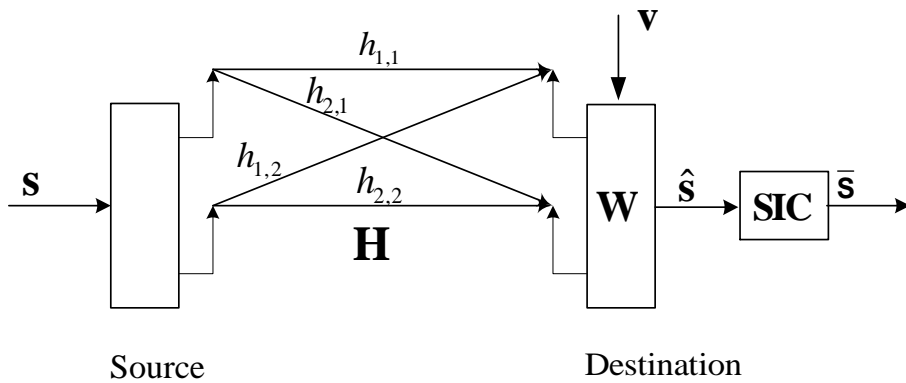


Figure 1.2: Block diagram of the equivalent MIMO channel.

In the following, we briefly review receiver algorithms for a single-hop MIMO system. For simplicity, we consider here a 2×2 MIMO transmission which essentially means both the transmitter and the receiver are equipped with two antennas (see Fig. 1.2). Thus, the received signal on the first receive antenna is

$$\begin{aligned} y_1 &= h_{1,1} s_1 + h_{1,2} s_2 + v_1 \\ &= \begin{bmatrix} h_{1,1} & h_{1,2} \end{bmatrix} \begin{bmatrix} s_1 \\ s_2 \end{bmatrix} + v_1 \end{aligned} \quad (1.1)$$

and that on the second receive antenna is

$$\begin{aligned} y_2 &= h_{2,1} s_1 + h_{2,2} s_2 + v_2 \\ &= \begin{bmatrix} h_{2,1} & h_{2,2} \end{bmatrix} \begin{bmatrix} s_1 \\ s_2 \end{bmatrix} + v_2 \end{aligned} \quad (1.2)$$

where y_1 and y_2 are the received symbols on the first and the second antennas respectively, $h_{j,i}$ is the channel from i th transmit antenna to j th receive antenna, s_1 and s_2 are the transmitted symbols, and v_1 and v_2 are the noises on first and second receive antennas respectively. For convenience, the above two equations can be combined in matrix notation as

$$\mathbf{y}_d = \mathbf{H}\mathbf{s} + \mathbf{v} \quad (1.3)$$

where $\mathbf{y}_d \triangleq \begin{bmatrix} y_1 \\ y_2 \end{bmatrix}$ is the received signal vector, $\mathbf{H} \triangleq \begin{bmatrix} h_{1,1} & h_{1,2} \\ h_{2,1} & h_{2,2} \end{bmatrix}$ is the MIMO channel matrix, $\mathbf{s} \triangleq \begin{bmatrix} s_1 \\ s_2 \end{bmatrix}$ is the source symbol vector, and $\mathbf{v} \triangleq \begin{bmatrix} v_1 \\ v_2 \end{bmatrix}$ is the additive Gaussian noise vector.

The ZF Algorithm

The first decoding technique to be described in this section is ZF. The ZF linear detector meeting the constraint $\mathbf{W}^H\mathbf{H} = \mathbf{I}_2$ is given by

$$\mathbf{W} = \mathbf{H}(\mathbf{H}^H\mathbf{H})^{-1}. \quad (1.4)$$

\mathbf{W}^H is also known as the pseudo-inverse of \mathbf{H} . Then the estimate for the transmit signal vector is

$$\hat{\mathbf{s}} = \mathbf{W}^H\mathbf{y}_d. \quad (1.5)$$

Using the ZF equalization approach described above, the receiver can obtain an estimate of the two transmitted symbols s_1 and s_2 as

$$\begin{bmatrix} \hat{s}_1 \\ \hat{s}_2 \end{bmatrix} = (\mathbf{H}^H\mathbf{H})^{-1}\mathbf{H}^H \begin{bmatrix} y_1 \\ y_2 \end{bmatrix} \quad (1.6)$$

where \hat{s}_1 and \hat{s}_2 are the estimates of s_1 and s_2 respectively.

The MMSE Algorithm

To estimate \mathbf{s} in (1.3) the MMSE approach tries to find a weight matrix \mathbf{W} that minimizes the statistical expectation of the signal estimation error given by

$$\text{tr}(\mathbf{E}[(\hat{\mathbf{s}} - \mathbf{s})(\hat{\mathbf{s}} - \mathbf{s})^H]) \quad (1.7)$$

Substituting (1.5) into (1.7), we find that the \mathbf{W} which minimizes (1.7) can be written as

$$\mathbf{W} = (\mathbf{H}\mathbf{H}^H + \mathbf{C}_v)^{-1}\mathbf{H} \quad (1.8)$$

where \mathbf{C}_v is the noise covariance matrix. Using the MMSE equalization approach described above, the receiver can obtain an estimate of the two transmitted symbols as

$$\begin{bmatrix} \hat{s}_1 \\ \hat{s}_2 \end{bmatrix} = \mathbf{H}^H (\mathbf{H}\mathbf{H}^H + \mathbf{C}_v)^{-1} \begin{bmatrix} y_1 \\ y_2 \end{bmatrix}. \quad (1.9)$$

The ZF and MMSE with SIC Algorithm

In the classical SIC algorithm, the receiver arbitrarily takes one of the estimated symbols, and subtracts its effect from the received symbols y_1 and y_2 (Fig. 1.3). However, a better BER performance can be achieved by choosing whether we should subtract the effect of \hat{s}_1 first or \hat{s}_2 first. To make this decision, let us find out the transmit symbol which comes at higher power at the receiver. The received power at both antennas corresponding to the transmitted symbol s_1 is

$$P_{s_1} = |h_{1,1}|^2 + |h_{2,1}|^2 \quad (1.10)$$

and the received power at both antennas corresponding to the transmitted symbol s_2 is

$$P_{s_2} = |h_{1,2}|^2 + |h_{2,2}|^2. \quad (1.11)$$

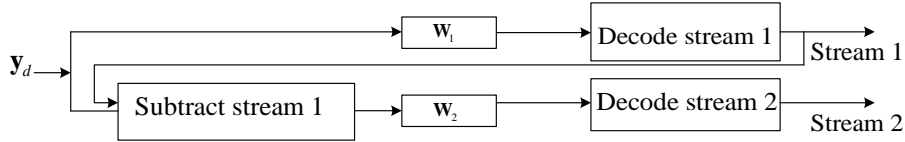


Figure 1.3: Successive interference cancellation technique.

Now, if $P_{s_1} > P_{s_2}$ then the receiver decides to remove the effect of \hat{s}_1 from the received signals y_1 and y_2 and obtain

$$\begin{bmatrix} r_1 \\ r_2 \end{bmatrix} = \begin{bmatrix} y_1 - h_{1,1}\hat{s}_1 \\ y_2 - h_{2,1}\hat{s}_1 \end{bmatrix}. \quad (1.12)$$

If there is no error propagation we can express the above equation in matrix notation as

$$\begin{bmatrix} r_1 \\ r_2 \end{bmatrix} = \begin{bmatrix} h_{1,2} \\ h_{2,2} \end{bmatrix} s_2 + \begin{bmatrix} v_1 \\ v_2 \end{bmatrix} \quad (1.13)$$

or equivalently as

$$\hat{\mathbf{r}}_2 = \mathbf{h}_2 s_2 + \mathbf{v}. \quad (1.14)$$

From (1.14), we can re-estimate s_2 as

$$\bar{s}_2 = \frac{\mathbf{h}_2^H \hat{\mathbf{r}}_2}{\mathbf{h}_2^H \mathbf{h}_2}. \quad (1.15)$$

Similarly, if $P_{s_2} > P_{s_1}$ then the receiver decides to remove the effect of \hat{s}_2 from the received signals y_1 and y_2 and then re-estimates \hat{s}_1 as

$$\begin{bmatrix} r_1 \\ r_2 \end{bmatrix} = \begin{bmatrix} y_1 - h_{1,2} \hat{s}_2 \\ y_2 - h_{2,2} \hat{s}_2 \end{bmatrix}. \quad (1.16)$$

If there is no error propagation we can express the above equation in matrix notation as

$$\begin{bmatrix} r_1 \\ r_2 \end{bmatrix} = \begin{bmatrix} h_{1,1} \\ h_{2,1} \end{bmatrix} s_1 + \begin{bmatrix} v_1 \\ v_2 \end{bmatrix} \quad (1.17)$$

or equivalently as

$$\hat{\mathbf{r}}_1 = \mathbf{h}_1 s_1 + \mathbf{v}. \quad (1.18)$$

From (1.18), we can re-estimate s_1 as

$$\bar{s}_1 = \frac{\mathbf{h}_1^H \hat{\mathbf{r}}_1}{\mathbf{h}_1^H \mathbf{h}_1}. \quad (1.19)$$

In this thesis, we focus on the MMSE receiver, since it performs better than the ZF receiver. We performed all the simulations in Matlab and used CVX toolbox wherever necessary [105].

1.4 Thesis Overview and Contributions

In this thesis, advanced algorithms for MIMO relay communication systems using parallel relays and SIC technique are presented considering non-regenerative relays. In Chapter 2, we study transmit beamforming and relay precoding design problem for parallel MIMO relay communication systems with distributed single-antenna relay nodes when a single data stream is transmitted from the source to destination node. In Chapter 3, we propose jointly optimal source precoding matrix and relay amplifying matrices for two-hop parallel MIMO relay communication systems with a linear minimum mean-squared error (LMMSE) receiver applied at the destination node. The projected gradient (PG) approach is applied to optimise the relay matrices where each relay has multiple antennas and multiple data streams are transmitted from the source to the destination node. To reduce the complexity of the algorithm in Chapter 3, we propose a simplified source and relay matrices design in Chapter 4 by relaxing power constraints at each relay node

to the power constraint at the output of the second-hop channel. In Chapter 5, we investigate ZF and MMSE receiver performance with and without using SIC technique in MIMO relay communication systems. We also investigate the optimal structure of the source precoding matrix and the relay amplifying matrices for parallel MIMO relay communication systems with multiple data streams when a nonlinear MMSE decision feedback equalizer (MMSE-DFE) receiver is used at the destination node. Chapter 6 summarizes the thesis and gives the outlook to some interesting future works.

Chapter 2: MIMO Transceiver Design with Distributed Relay Nodes

In this chapter, we study the optimal transmit beamforming vector and the relay amplifying factors design problem of parallel MIMO relay communication systems with distributed single-antenna relay nodes when a single data stream is transmitted from the source to destination node. We propose a jointly optimal iterative source and relay beamforming algorithm which minimizes the mean-squared error (MSE) of the signal waveform estimation for single-antenna relay nodes in a parallel MIMO relay communication system. Compared with the existing techniques, the proposed algorithm performs much better in terms of bit-error-rate (BER) and MSE of signal waveform estimation at the destination node.

The material in Chapter 2 is based on the conference publication:

- A. Toding, M. R. A. Khandaker, and Y. Rong, “Joint Source and Relay Optimization for Distributed MIMO Relay System”, in *Proc. 17th Asia-Pacific Conference on Communications (APCC’2011)*, Sabah, Malaysia, Oct. 2-5, 2011, pp. 604-608.

In Chapters 3-5, we investigate optimal source and relay matrices design for MIMO relay communication systems with multiple parallel relay nodes when multiple parallel data streams are transmitted from source to destination node.

Chapter 3: Parallel MIMO Relay Design Based on Linear Receiver

We propose jointly optimal source precoding matrix and relay amplifying matrices for two-hop parallel MIMO relay communication systems with multiple parallel data streams when a linear receiver is applied at the destination node considering individual transmission power constraint at each relay node. We derive the structure of the optimal relay matrices and develop an iterative algorithm to jointly optimize the source and relay matrices to minimize the MSE of the signal waveform estimation at the destination node using the PG approach.

The material in Chapter 3 is based on the journal submission:

- A. Toding, M. R. A. Khandaker, and Y. Rong, “Joint Source and Relay Design for MIMO Multi-Relay Systems Using Projected Gradient Approach”, *EURASIP Journal on Wireless Commun. Network.*, submitted, Aug. 2013.

Chapter 4: Simplified Source and Relay Matrices Design

To reduce the complexity of the algorithm in Chapter 3, we first relax the power constraint at each relay node to the power constraint at the output of the second-hop channel. After solving the relaxed optimisation problem, the relay matrices are then scaled to satisfy the individual power constraint at each relay node. Compared with the second part of the thesis, the algorithm in Chapter 4 has an improved performance-complexity tradeoff.

The material in Chapter 4 is based on the journal publication:

- A. Toding, M. R. A. Khandaker, and Y. Rong, “Joint Source and Relay Optimization for Parallel MIMO Relay Networks”, *EURASIP Journal on Advances in Signal Processing*, 2012:174.

and the conference publication:

- A. Toding, M. R. A. Khandaker, and Y. Rong, “Optimal Joint Source and Relay Beamforming for Parallel MIMO Relay Networks”, in *Proc. 6th Int. Conf. Wireless Commun., Networking and Mobile Computing (WiCOM'2010)*, Chengdu, China, Sep. 23-25, 2010.

Chapter 5: Parallel MIMO Relay Design Based on Nonlinear Receiver

We investigate the optimal structure of the source precoding matrix and the relay amplifying matrices for parallel MIMO relay communication systems with multiple parallel data streams when a nonlinear MMSE-DFE receiver is used at the destination node. The MMSE criterion is used to detect the transmitted signal at each stream. We show that the optimal source precoding matrix and the optimal relay amplifying matrices have a beamforming structure. By using such optimal source and relay matrices and the MMSE-DFE receiver, a joint source and relay power loading algorithm is developed to minimize the MSE of the signal waveform estimation.

The material in Chapter 5 is based on the journal publication:

- A. Toding, M. R. A. Khandaker, and Y. Rong, “Joint Source and Relay Optimization for Parallel MIMO Relay Networks”, *EURASIP Journal on Advances in Signal Processing*, 2012:174.

and the conference publications:

- A. Toding, M. R. A. Khandaker, and Y. Rong, “Joint Source and Relay Optimization for Parallel MIMO Relays Using MMSE-DFE Receiver”, in *Proc. 16th Asia-Pacific Conference on Communications (APCC'2010)*, Auckland, New Zealand, Nov. 1-3, 2010, pp. 12-16.
- A. Toding and Y. Rong, “Investigating Successive Interference Cancellation in MIMO Relay Network”, in *Proc. IEEE TENCON*, Bali, Indonesia, Nov. 21-24, 2011, pp. 359-363.

Chapter 2

MIMO Transceiver Design with Distributed Relay Nodes

In this chapter, we study the optimal transmit beamforming vector and the relay amplifying factors design problem for a parallel MIMO relay communication system with distributed single-antenna relay nodes when a single data stream is transmitted from the source to destination node. By using the optimal beamforming vector, an iterative joint source and relay beamforming algorithm is developed to minimize the MSE of the signal waveform estimation. In Section 2.1, we give a brief overview of existing works. The system model of a parallel MIMO relay communication system with distributed single-antenna relay nodes is introduced in Section 2.2. In Section 2.3, we develop the jointly optimal source and relay algorithm. Section 2.4 shows the simulation results. The chapter is briefly summarized in Section 2.5.

2.1 Overview of Single-Antenna Relay Technique

In wireless communications, signal fading and shadowing effects are very common phenomena that degrade the system performance. An efficient way to address this issue is to transmit signals through one or multiple relays [1–23]. Introducing multiple antennas at transmitting and receiving ends, which we call MIMO relay communication systems, can provide further improvement in terms of both spectral efficiency and link reliability [37, 47]. Many works have studied the optimal relay amplifying matrix for MIMO relay channels. In [12] and [54], the optimal relay amplifying matrix is designed to maximize

the MI between the source node and the destination node, assuming that the source covariance matrix is an identity matrix. In [57] and [58], the optimal relay amplifying matrix was designed to minimize the MSE of the signal waveform estimation at the destination node.

However, few researches have studied the jointly optimal source precoding matrix and the relay amplifying matrix for the source-relay-destination channel. In [60], a unified framework was developed to jointly optimize the source precoding matrix and the relay amplifying matrix for a broad class of objective functions. In [59], the source covariance matrix and the relay amplifying matrix were jointly designed to maximize the source-destination MI. All the works [12, 37, 47, 54, 57–60] focus on MIMO relay systems with a single relay node at each hop. In [38] and [89], the optimal source and relay matrices were designed for a multi-hop MIMO relay network with serial relays.

MIMO relay communication systems with multiple parallel relay nodes have been investigated in [73, 74]. In [74], the authors investigated the jointly optimal structure of the source precoding matrix and the relay amplifying matrices considering a linear MMSE receiver at the destination node. On the other hand, a distributed relay network is investigated in [29] where multiple users and relays, each having a single-antenna, are considered.

In this chapter, we propose a jointly optimal source and relay beamforming algorithm which minimizes the MSE of the signal waveform estimation for single-antenna relay nodes in a MIMO relay communication system. In contrast to [73, 74], where the receive power constraint at the destination node is considered, we consider in this chapter the sum transmit power constraint throughout all relay nodes.

2.2 Distributed MIMO Relay System Model

Fig. 2.1 illustrates a two-hop parallel MIMO relay communication system consisting of one source node, K parallel relay nodes, and one destination node. We assume that the source and the destination nodes have N_s and N_d antennas, respectively, whereas each relay node has a single-antenna. Due to its merit of simplicity, we consider the amplify-and-forward scheme at each relay. The communication process between the source and destination nodes is completed in two time slots. In the first time slot, the modulated symbol s is linearly precoded as

$$\mathbf{x} = \mathbf{b}s \tag{2.1}$$

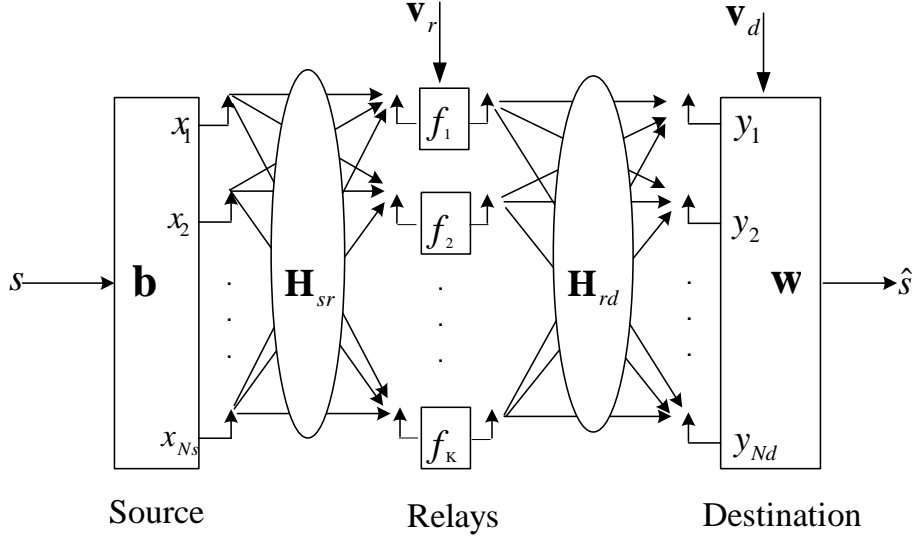


Figure 2.1: Block diagram of a parallel MIMO relay communication system with a single data stream.

where \mathbf{b} is an $N_s \times 1$ transmit beamforming vector. The precoded vector \mathbf{x} is then transmitted to the relay nodes. The received signal at the i th relay node can be written as

$$y_{r,i} = \mathbf{h}_{sr,i} \mathbf{x} + v_{r,i}, \quad i = 1, \dots, K \quad (2.2)$$

where $\mathbf{h}_{sr,i}$ is the $1 \times N_s$ channel vector between the source and the i th relay node, $y_{r,i}$ and $v_{r,i}$ are the received signal and the additive Gaussian noise at the i th relay node, respectively.

In the second time slot, the source node is silent, while each relay node transmits the amplified signal to the destination node as

$$x_{r,i} = f_i y_{r,i}, \quad i = 1, \dots, K \quad (2.3)$$

where f_i is the amplifying coefficient at the i th relay node. The received signal vector at the destination node can be written as

$$\mathbf{y}_d = \sum_{i=1}^K \mathbf{h}_{rd,i} x_{r,i} + \mathbf{v}_d \quad (2.4)$$

where $\mathbf{h}_{rd,i}$ is the $N_d \times 1$ channel vector between the i th relay and the destination node, \mathbf{y}_d and \mathbf{v}_d are the received signal and the additive Gaussian noise vector at the destination node, respectively.

Substituting (2.1)-(2.3) into (2.4), we have

$$\begin{aligned} \mathbf{y}_d &= \sum_{i=1}^K (\mathbf{h}_{rd,i} f_i \mathbf{h}_{sr,i} \mathbf{b}_s + \mathbf{h}_{rd,i} f_i v_{r,i}) + \mathbf{v}_d \\ &= \mathbf{H}_{rd} \mathbf{F} \mathbf{H}_{sr} \mathbf{b}_s + \mathbf{H}_{rd} \mathbf{F} \mathbf{v}_r + \mathbf{v}_d \end{aligned} \quad (2.5)$$

where we define

$$\begin{aligned} \mathbf{H}_{sr} &\triangleq [\mathbf{h}_{sr,1}^T, \mathbf{h}_{sr,2}^T, \dots, \mathbf{h}_{sr,K}^T]^T \\ \mathbf{H}_{rd} &\triangleq [\mathbf{h}_{rd,1}, \mathbf{h}_{rd,2}, \dots, \mathbf{h}_{rd,K}] \\ \mathbf{F} &\triangleq \text{diag}([f_1, f_2, \dots, f_K]^T) \\ \mathbf{v}_r &\triangleq [v_{r,1}, v_{r,2}, \dots, v_{r,K}]^T. \end{aligned}$$

Here \mathbf{H}_{sr} is a $K \times N_s$ channel matrix between the source node and all relay nodes, \mathbf{H}_{rd} is an $N_d \times K$ channel matrix between all relay nodes and the destination node, \mathbf{F} is a $K \times K$ diagonal equivalent relay matrix, and \mathbf{v}_r is obtained by stacking the noise terms at all the relays. We assume that all noises are independent and identically distributed (i.i.d.) with zero mean and unit variance.

The diagram of the equivalent MIMO relay system with a single data stream described by (2.5) is shown in Fig. 2.2. The received signal vector at the destination node can be equivalently written as

$$\mathbf{y}_d = \bar{\mathbf{h}} \mathbf{s} + \bar{\mathbf{v}}$$

where we define $\bar{\mathbf{h}} \triangleq \mathbf{H}_{rd} \mathbf{F} \mathbf{H}_{sr} \mathbf{b}$ as the effective MIMO channel vector of the source-relay-destination link, and $\bar{\mathbf{v}} \triangleq \mathbf{H}_{rd} \mathbf{F} \mathbf{v}_r + \mathbf{v}_d$ as the equivalent noise vector.

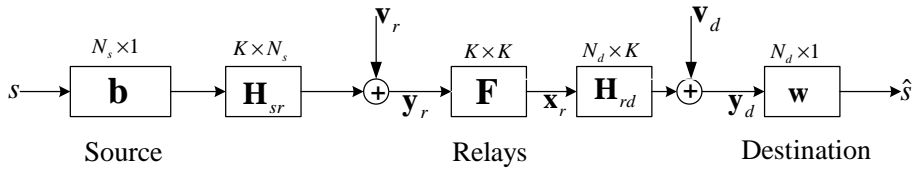


Figure 2.2: Block diagram of the equivalent MIMO relay system with a single data stream.

2.3 Optimal Source and Relay Design

In this section we develop the optimal transmit beamforming vector \mathbf{b} and the relay amplifying matrix \mathbf{F} to minimize the MSE of the signal waveform estimation. By using

a linear receiver, the estimated signal waveform vector at the destination node is given by

$$\hat{s} = \mathbf{w}^H \mathbf{y}_d \quad (2.6)$$

where \mathbf{w} is an $N_d \times 1$ weight vector.

The MMSE approach tries to find a weight vector \mathbf{w} that minimizes the statistical expectation of the signal waveform estimation given by

$$\text{MSE} = \text{E}[|\hat{s} - s|^2]. \quad (2.7)$$

We assume that the source signal satisfies $\text{E}[|s|^2] = 1$. Substituting (2.6) into (2.7), we find that the \mathbf{w} which minimizes (2.7) can be written as

$$\mathbf{w} = (\bar{\mathbf{h}}\bar{\mathbf{h}}^H + \mathbf{C}_{\bar{v}})^{-1}\bar{\mathbf{h}} \quad (2.8)$$

where $\mathbf{C}_{\bar{v}}$ is the equivalent noise covariance matrix given by

$$\begin{aligned} \mathbf{C}_{\bar{v}} &= \text{E}[\bar{\mathbf{v}}\bar{\mathbf{v}}^H] \\ &= \mathbf{H}_{rd}\mathbf{F}\mathbf{F}^H\mathbf{H}_{rd}^H + \mathbf{I}_{N_d}. \end{aligned} \quad (2.9)$$

Substituting (2.8) back into (2.7), we obtain the minimal MSE as a function of \mathbf{b} and \mathbf{F} , given by

$$\text{MSE} = 1 - \bar{\mathbf{h}}^H (\bar{\mathbf{h}}\bar{\mathbf{h}}^H + \mathbf{C}_{\bar{v}})^{-1} \bar{\mathbf{h}}. \quad (2.10)$$

Applying the matrix inversion lemma $(\mathbf{A} + \mathbf{BCD})^{-1} = \mathbf{A}^{-1} - \mathbf{A}^{-1}\mathbf{B}(\mathbf{DA}^{-1}\mathbf{B} + \mathbf{C}^{-1})^{-1}\mathbf{DA}^{-1}$, (2.10) can be written as

$$\text{MSE} = (1 + \bar{\mathbf{h}}^H \bar{\mathbf{C}}_{\bar{v}}^{-1} \bar{\mathbf{h}})^{-1}. \quad (2.11)$$

From (2.3), the total transmission power consumed by all the relay nodes can be expressed as

$$\text{tr}(\text{E}[\mathbf{x}_r \mathbf{x}_r^H]) = \text{tr}(\mathbf{F} [\mathbf{H}_{sr} \mathbf{b} \mathbf{b}^H \mathbf{H}_{sr}^H + \mathbf{I}_K] \mathbf{F}^H). \quad (2.12)$$

By using (2.12), the joint source and relay optimization problem can be formulated as

$$\min_{\mathbf{F}, \mathbf{b}} \text{MSE} \quad (2.13)$$

$$\text{s.t. } \mathbf{b}^H \mathbf{b} \leq P_s \quad (2.14)$$

$$\text{tr}(\mathbf{F} [\mathbf{H}_{sr} \mathbf{b} \mathbf{b}^H \mathbf{H}_{sr}^H + \mathbf{I}_K] \mathbf{F}^H) \leq P_r \quad (2.15)$$

where (2.14) is the transmit power constraint at the source node, and (2.15) is the sum transmit power constraint throughout all relay nodes. Here $P_r > 0$ and $P_s > 0$ are the corresponding power budget. The problem (2.13)-(2.15) is highly nonconvex and a closed-form expression of the optimal \mathbf{F} and \mathbf{b} is intractable. In the following, we develop an iterative algorithm to optimize \mathbf{F} and \mathbf{b} .

2.3.1 Optimal Relay Factors

For given beamforming vector \mathbf{b} satisfying (2.14), we optimize the relay matrix \mathbf{F} by solving the following optimization problem

$$\min_{\mathbf{F}} \text{MSE} \quad (2.16)$$

$$\text{s.t. } \text{tr}(\mathbf{F}[\mathbf{H}_{sr}\mathbf{b}\mathbf{b}^H\mathbf{H}_{sr}^H+\mathbf{I}_K]\mathbf{F}^H) \leq P_r. \quad (2.17)$$

Let us introduce

$$\bar{\mathbf{h}}_s \triangleq \mathbf{H}_{sr}\mathbf{b}. \quad (2.18)$$

Substituting (2.18) back into (2.16)-(2.17), we can rewrite the optimization problem as

$$\min_{\mathbf{F}} [1+\bar{\mathbf{h}}_s^H\mathbf{F}^H\mathbf{H}_{rd}^H(\mathbf{H}_{rd}\mathbf{F}\mathbf{F}^H\mathbf{H}_{rd}^H+\mathbf{I}_{N_d})^{-1}\mathbf{H}_{rd}\mathbf{F}\bar{\mathbf{h}}_s]^{-1} \quad (2.19)$$

$$\text{s.t. } \sum_{i=1}^K |f_i|^2 (|\bar{h}_{s,i}|^2 + 1) \leq P_r. \quad (2.20)$$

The problem (2.19)-(2.20) is equivalent to

$$\max_{\mathbf{F}} \bar{\mathbf{h}}_s^H\mathbf{F}^H\mathbf{H}_{rd}^H(\mathbf{H}_{rd}\mathbf{F}\mathbf{F}^H\mathbf{H}_{rd}^H+\mathbf{I}_{N_d})^{-1}\mathbf{H}_{rd}\mathbf{F}\bar{\mathbf{h}}_s \quad (2.21)$$

$$\text{s.t. } \sum_{i=1}^K |f_i|^2 (|\bar{h}_{s,i}|^2 + 1) \leq P_r. \quad (2.22)$$

Since the objective function (2.21) is still a complicated function of \mathbf{F} , in the following, we optimize an upper-bound of (2.21). The problem can be rewritten as

$$\max_{\mathbf{F}} \bar{\mathbf{h}}_s^H\mathbf{F}^H\mathbf{H}_{rd}^H\mathbf{H}_{rd}\mathbf{F}\bar{\mathbf{h}}_s \quad (2.23)$$

$$\text{s.t. } \sum_{i=1}^K |f_i|^2 (|\bar{h}_{s,i}|^2 + 1) \leq P_r. \quad (2.24)$$

Let $\mathbf{f} \triangleq [f_1, f_2, \dots, f_K]^T$ denote the diagonal elements of \mathbf{F} and define $\mathbf{D}_s \triangleq \text{diag}(\bar{\mathbf{h}}_s)$, so that

$$\mathbf{F}\bar{\mathbf{h}}_s = \mathbf{D}_s\mathbf{f}. \quad (2.25)$$

Now by substituting (2.25) in (2.23)-(2.24), we can express the maximization problem as follows

$$\max_{\mathbf{f}} \mathbf{f}^H \mathbf{D}_s^H \mathbf{H}_{rd}^H \mathbf{H}_{rd} \mathbf{D}_s \mathbf{f} \quad (2.26)$$

$$\text{s.t. } \mathbf{f}^H \mathbf{A} \mathbf{f} \leq P_r \quad (2.27)$$

where $\mathbf{A} \triangleq \mathbf{D}_s \mathbf{D}_s^H + \mathbf{I}_K$. Defining $\bar{\mathbf{f}} \triangleq \mathbf{A}^{\frac{1}{2}} \mathbf{f}$, the problem (2.26)-(2.27) can be equivalently written as

$$\begin{aligned} \max_{\bar{\mathbf{f}}} \quad & \bar{\mathbf{f}}^H \mathbf{A}^{-\frac{H}{2}} \mathbf{D}_s^H \mathbf{H}_{rd}^H \mathbf{H}_{rd} \mathbf{D}_s \mathbf{A}^{-\frac{1}{2}} \bar{\mathbf{f}} \\ \text{s.t.} \quad & \bar{\mathbf{f}}^H \bar{\mathbf{f}} \leq P_r. \end{aligned}$$

Introducing $\mathbf{Z} \triangleq \mathbf{A}^{-\frac{H}{2}} \mathbf{D}_s^H \mathbf{H}_{rd}^H \mathbf{H}_{rd} \mathbf{D}_s \mathbf{A}^{-\frac{1}{2}}$, we obtain

$$\max_{\bar{\mathbf{f}}} \bar{\mathbf{f}}^H \mathbf{Z} \bar{\mathbf{f}} \quad (2.28)$$

$$\text{s.t. } \bar{\mathbf{f}}^H \bar{\mathbf{f}} \leq P_r. \quad (2.29)$$

The Lagrangian of the optimization problem (2.28)-(2.29) can be written as

$$\mathcal{L} = -\bar{\mathbf{f}}^H \mathbf{Z} \bar{\mathbf{f}} + \mu_1 (\bar{\mathbf{f}}^H \bar{\mathbf{f}} - P_r) \quad (2.30)$$

where $\mu_1 \geq 0$ is the Lagrangian multiplier associated with the constraint (2.29). Taking the derivative of \mathcal{L} with respect to $\bar{\mathbf{f}}^H$ and letting the result be 0, it can be shown that the optimal $\bar{\mathbf{f}}$ satisfies the following equation

$$\mathbf{Z} \bar{\mathbf{f}} = \mu_1 \bar{\mathbf{f}}.$$

Thus $\bar{\mathbf{f}} = \sqrt{P_r} \text{eig}(\mathbf{Z})$, where $\text{eig}(\mathbf{Z})$ stands for the principal eigenvector of \mathbf{Z} .

2.3.2 Joint Source and Relay Optimization Algorithm

For a fixed \mathbf{F} , the problem (2.13) - (2.15) can be expressed as below to optimize the beamforming vector \mathbf{b}

$$\min_{\mathbf{b}} (1 + \mathbf{b}^H \boldsymbol{\Psi}_1 \mathbf{b})^{-1} \quad (2.31)$$

$$\text{s.t. } \mathbf{b}^H \mathbf{b} \leq P_s \quad (2.32)$$

$$\mathbf{b}^H \boldsymbol{\Psi}_2 \mathbf{b} \leq \bar{P}_r \quad (2.33)$$

where we define

$$\Psi_1 \triangleq \mathbf{H}_{sr}^H \mathbf{F}^H \mathbf{H}_{rd}^H \mathbf{H}_{rd} \mathbf{F} \mathbf{H}_{sr}$$

$$\Psi_2 \triangleq \mathbf{H}_{sr}^H \mathbf{F}^H \mathbf{F} \mathbf{H}_{sr}$$

$$\bar{P}_r \triangleq P_r - \text{tr}(\mathbf{F}\mathbf{F}^H).$$

The problem (2.31)-(2.33) is equivalent to

$$\max_{\mathbf{b}} \mathbf{b}^H \Psi_1 \mathbf{b} \quad (2.34)$$

$$\text{s.t. } \mathbf{b}^H \mathbf{b} \leq P_s \quad (2.35)$$

$$\mathbf{b}^H \Psi_2 \mathbf{b} \leq \bar{P}_r. \quad (2.36)$$

The Lagrangian function associated with the problem (2.34)-(2.36) can be written as

$$\mathcal{L} = -\mathbf{b}^H \Psi_1 \mathbf{b} + \mu_2 (\mathbf{b}^H \mathbf{b} - P_s) + \mu_3 (\mathbf{b}^H \Psi_2 \mathbf{b} - \bar{P}_r). \quad (2.37)$$

Here $\mu_2 \geq 0$ and $\mu_3 \geq 0$ are the Lagrangian multipliers associated with the constraints (2.35) and (2.36), respectively. The problem (2.34)-(2.36) can be solved by using KKT conditions [106] that can be expressed as

$$\frac{\partial \mathcal{L}}{\partial \mathbf{b}^H} = 0 \quad (2.38)$$

$$\mu_2 (\mathbf{b}^H \mathbf{b} - P_s) = 0 \quad (2.39)$$

$$\mu_3 (\mathbf{b}^H \Psi_2 \mathbf{b} - \bar{P}_r) = 0 \quad (2.40)$$

$$\mathbf{b}^H \mathbf{b} \leq P_s \quad (2.41)$$

$$\mathbf{b}^H \Psi_2 \mathbf{b} \leq \bar{P}_r \quad (2.42)$$

$$\mu_2 \geq 0, \quad \mu_3 \geq 0. \quad (2.43)$$

Now we set out to solve (2.38)-(2.43). If $\mu_2 > 0$ and $\mu_3 = 0$, then the optimization problem (2.34)-(2.36) can be rewritten as

$$\max_{\mathbf{b}} \mathbf{b}^H \Psi_1 \mathbf{b} \quad (2.44)$$

$$\text{s.t. } \mathbf{b}^H \mathbf{b} = P_s. \quad (2.45)$$

Thus we solve \mathbf{b} as

$$\mathbf{b} = \sqrt{P_s} \text{eig}(\Psi_1). \quad (2.46)$$

If \mathbf{b} in (2.46) satisfies the constraint (2.36), then (2.46) is the optimal solution to the problem (2.34)-(2.36). Otherwise, if $\mu_3 > 0$ and $\mu_2 = 0$, then the optimization problem (2.34)-(2.36) can be rewritten as

$$\max_{\mathbf{b}} \mathbf{b}^H \Psi_1 \mathbf{b} \quad (2.47)$$

$$\text{s.t. } \mathbf{b}^H \Psi_2 \mathbf{b} = \bar{P}_r. \quad (2.48)$$

Then we solve \mathbf{b} as

$$\mathbf{b} = \alpha \text{eig}(\Psi_2^{-1} \Psi_1) \quad (2.49)$$

where $\alpha = \sqrt{\bar{P}_r / (\text{eig}^H(\Psi_2^{-1} \Psi_1) \Psi_2 \text{eig}(\Psi_2^{-1} \Psi_1))}$. If \mathbf{b} in (2.49) satisfies the constraint (2.35), then (2.49) is the optimal solution to the problem (2.34)-(2.36).

Finally, if $\mu_2 > 0$ and $\mu_3 > 0$, then we have from (2.38) that

$$\Psi_1 \mathbf{b} = \mu_2 \mathbf{b} + \mu_3 \Psi_2 \mathbf{b}$$

which can be equivalently written as

$$\left(\mathbf{I}_{N_s} + \frac{\mu_3}{\mu_2} \Psi_2 \right)^{-1} \Psi_1 \mathbf{b} = \mu_2 \mathbf{b}. \quad (2.50)$$

Thus the optimal \mathbf{b} can be obtained as

$$\mathbf{b} = \sqrt{\bar{P}_s} \text{eig}((\mathbf{I}_{N_s} + \lambda \Psi_2)^{-1} \Psi_1) \quad (2.51)$$

where $\lambda > 0$ can be found by substituting (2.51) back into (2.48) and solving the obtained nonlinear equation.

Table 2.1: Procedure of solving the problem (2.13) - (2.15) by the proposed iterative algorithm.

1. Initialize the algorithm with random $\mathbf{b}^{(0)}$; Set $n = 0$.
2. Solve the subproblem (2.26)-(2.27) using given $\mathbf{b}^{(n)}$ to obtain $\mathbf{f}^{(n)}$.
3. Solve the subproblem (2.34)-(2.36) using $\mathbf{F}^{(n)}$ to obtain $\mathbf{b}^{(n)}$.
4. If $\max \text{abs} \|\mathbf{b}^{(n+1)} - \mathbf{b}^{(n)}\| \leq \varepsilon$, then end.
Otherwise, let $n := n + 1$ and go to step 2.

Now the original problem (2.13)-(2.15) can be solved in an iterative fashion. In each iteration, we first fix \mathbf{b} and update \mathbf{f} by solving the problem (2.26)-(2.27). Then we update \mathbf{b} with \mathbf{F} fixed through solving the problem (2.34)-(2.36). The procedure of the proposed iterative algorithm is listed in Table 2.1, where ε is a small positive number close to zero. Since each update may only reduce or maintain, but can not increase the MSE, a monotonic convergence of this iterative algorithm follows directly from this observation.

2.4 Numerical Examples

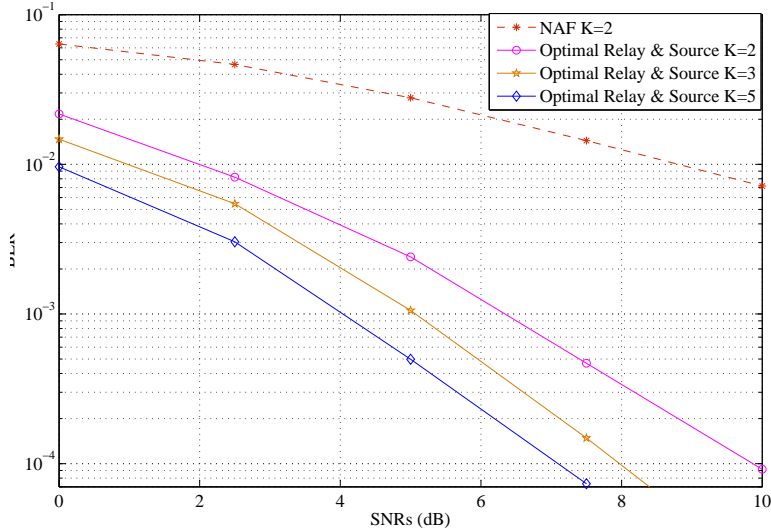


Figure 2.3: Example 2.1 BER versus SNR_s with varying K . $N_s = N_d = 3$, $\text{SNR}_r = 20\text{dB}$.

In this section, we study the performance of the proposed optimal transmit beamforming vector and the relay amplifying factors for a parallel MIMO relay communication system with distributed single-antenna relay nodes when a single data stream is transmitted from the source to destination node. We compare the performance of the proposed algorithm with the naive amplify-and-forward (NAF) scheme in terms of BER. For the NAF scheme, we define source and relay matrices as scaled identity matrices satisfying the power constraints. All simulations are conducted in a flat Rayleigh fading environment using binary phase shift keying (BPSK) constellations, and the noises are i.i.d. Gaussian random variables with zero mean and unit variance. The channel

matrices have zero-mean entries with variances σ_s^2/N_s and σ_r^2/K for \mathbf{H}_{sr} and \mathbf{H}_{rd} , respectively. We vary the SNR in the source-to-relay link (SNR_s) while fixing the SNR in the relay-to-destination link (SNR_r) to 20dB. We transmit 1000 randomly generated bits in each channel realization, and the BER results are averaged through 200 random channel realizations.

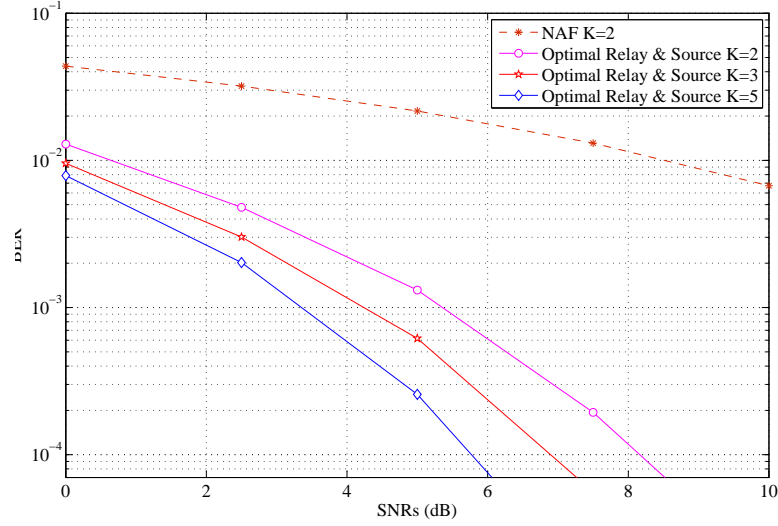


Figure 2.4: Example 2.2 BER versus SNR_s with varying K . $N_s = N_d = 5$, $\text{SNR}_r = 20\text{dB}$.

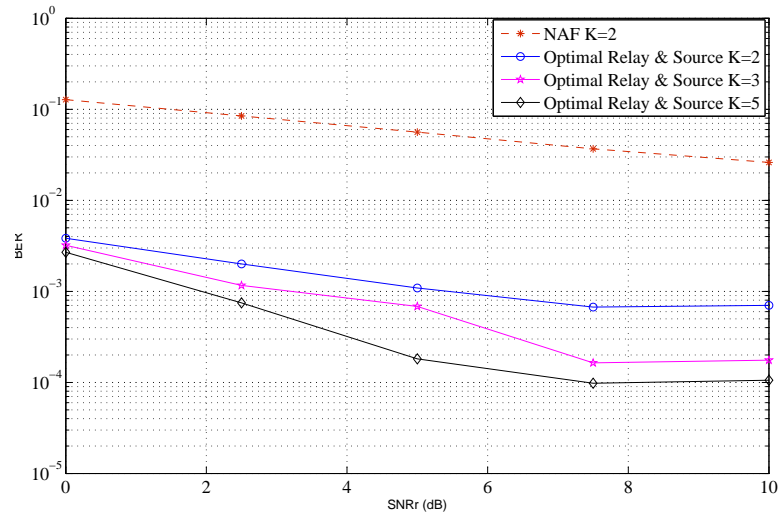


Figure 2.5: Example 2.3 BER versus SNR_r with varying K . $N_s = N_d = 3$, $\text{SNR}_s = 20\text{dB}$.

In the first example, we study the effect of the number of relays to the system BER

performance using the proposed algorithm. We choose $N_s = N_d = 3$. Fig. 2.3 shows the BER performance with $K = 2, 3$, and 5. It can be seen that at $\text{BER} = 10^{-3}$, we achieve a 2.5dB gain by increasing from $K = 2$ to $K = 5$.

In the second example, we simulate a MIMO relay communication system with distributed single-antenna relay nodes with $N_s = N_d = 5$. Fig. 2.4 shows the BER performance with $K = 2, 3$, and 5. It can be seen that at $\text{BER} = 10^{-3}$, we achieve a 2dB gain by increasing from $K = 2$ to $K = 5$.

In the last example, we study the effect of the number of relays to the system BER performance versus SNR_r . We choose $N_s = N_d = 3$. Fig. 2.5 shows the BER performance of the algorithms with $K = 2, 3$, and 5. It can be seen that at $\text{BER} = 10^{-3}$, we achieve a 3dB gain by increasing from $K = 2$ to $K = 5$.

Table 2.2 indicates how fast the proposed iterative algorithm converges. The number of iterations required in a typical run to converge up to $\varepsilon = 10^{-3}$ is shown in the table. Here we set $N_s = N_d = 3$, $K = 2$.

Table 2.2: Iterations required till convergence in the proposed algorithm

| | | | | | | |
|---------------------|---|---|---|---|---|----|
| SNR_s (dB) | 0 | 2 | 4 | 6 | 8 | 10 |
| Iterations required | 2 | 3 | 3 | 4 | 5 | 5 |

2.5 Chapter Summary

In this chapter, we have studied the optimal transmit beamforming vector and the relay amplifying factors design problem of a parallel MIMO relay communication system with distributed single-antenna relay nodes when a single data stream is transmitted from the source to destination node. The proposed joint source and relay beamforming algorithm provides an improved performance.

Chapter 3

Parallel MIMO Relay Design Based on Linear Receiver

In this chapter, we develop the optimal source precoding matrix and relay amplifying matrices for two-hop non-regenerative MIMO multi-relay systems with multiple data streams when a linear MMSE receiver is used at the destination node. We provide an overview of existing works in Section 3.1. In Section 3.2, the parallel MIMO relay system model is introduced. We show in Section 3.3 that the optimal relay amplifying matrices have a beamforming structure. Exploiting the structure of relay matrices, an iterative joint source and relay matrices optimization algorithm is developed to minimize the MSE of the signal waveform estimation at the destination node using the PG approach. The performance of the proposed algorithm is demonstrated through numerical simulations in Section 3.4. Finally, the chapter is summarized in Section 3.5.

3.1 Existing Works with Linear MMSE Receiver

Recently, MIMO relay communication systems have attracted much research interest and provided significant improvement in terms of both spectral efficiency and link reliability [3, 12, 38, 54, 57–60, 69, 73, 75]. Many works have studied the optimal relay amplifying matrix for the source-relay-destination channel. In [12, 54], the optimal relay amplifying matrix maximizing the mutual information (MI) between the source and destination nodes was derived assuming that the source covariance matrix is an identity

matrix. In [57, 69], the optimal relay amplifying matrix was designed to minimize MSE of the signal waveform estimation at the destination node.

A few researches have studied the joint optimization of the source precoding matrix and the relay amplifying matrix for the source-relay-destination channel. In [59], both the source and relay matrices were jointly designed to maximize the source-destination MI. In [38, 60], source and relay matrices were developed to jointly optimize a broad class of objective functions. The author of [75], investigated the joint source and relay optimization for two-way MIMO relay systems using the projected gradient (PG) approach. All the works in [3, 12, 38, 54, 57–60, 69, 75] considered a single relay node at each hop. The authors of [73] developed the optimal relay amplifying matrices with multiple relay nodes. In Chapter 2, we proposed a jointly optimal source and relay beamforming algorithm which minimizes the MSE of the signal waveform estimation for single-antenna relay nodes in a MIMO relay communication system.

In this chapter, we propose a jointly optimal source precoding matrix and relay amplifying matrices design for a two-hop non-regenerative MIMO relay communication system with multiple relay nodes using the PG approach. We show that the optimal relay amplifying matrices have a beamforming structure. This result generalizes the optimal source and relay matrices design from a single relay node case [60] to multiple parallel relay nodes scenario. Exploiting the structure of relay matrices, an iterative joint source and relay matrices optimization algorithm is developed to minimize the MSE of the signal waveform estimation. Different to Chapter 2, in this chapter, we study the optimal source and relay matrices which minimize the MSE of the signal waveform estimation of multiple data streams with multi-antenna relay nodes. Simulation results demonstrate the effectiveness of the proposed iterative joint source and relay matrices design algorithm with multiple parallel relay nodes using the PG approach.

3.2 Parallel MIMO Relay System

In this section, we introduce the model of a two-hop parallel MIMO relay communication system consisting of one source node, K parallel relay nodes, and one destination node with multiple data streams as shown in Fig. 3.1. We assume that the source and destination nodes have N_s and N_d antennas, respectively, and each relay node has N_r antennas. The generalization to systems with different number of antennas at each

relay node is straightforward. Due to its merit of simplicity, a linear non-regenerative strategy is applied at each relay node.

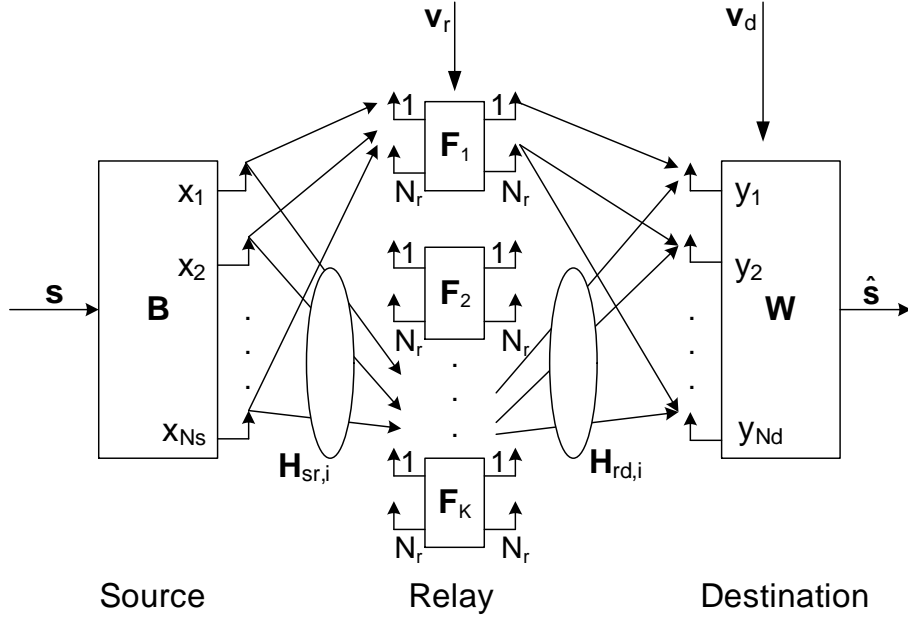


Figure 3.1: Block diagram of a parallel MIMO relay communication system with multiple data streams.

The communication process between the source and destination nodes is completed in two time slots. In the first time slot, the $N_b \times 1$ modulated source symbol vector \mathbf{s} is linearly precoded as

$$\mathbf{x} = \mathbf{B} \mathbf{s} \quad (3.1)$$

where \mathbf{B} is an $N_s \times N_b$ source precoding matrix. We assume that the source signal vector satisfies $E[\mathbf{s}\mathbf{s}^H] = \mathbf{I}_{N_b}$. The precoded vector \mathbf{x} is transmitted to K parallel relay nodes. The $N_r \times 1$ received signal vector at the i th relay node can be written as

$$\mathbf{y}_{r,i} = \mathbf{H}_{sr,i} \mathbf{x} + \mathbf{v}_{r,i}, \quad i = 1, \dots, K \quad (3.2)$$

where $\mathbf{H}_{sr,i}$ is the $N_r \times N_s$ MIMO channel matrix between the source and the i th relay nodes and $\mathbf{v}_{r,i}$ is the additive Gaussian noise vector at the i th relay node.

In the second time slot, the source node is silent, while each relay node transmits the linearly amplified signal vector to the destination node as

$$\mathbf{x}_{r,i} = \mathbf{F}_i \mathbf{y}_{r,i}, \quad i = 1, \dots, K \quad (3.3)$$

where \mathbf{F}_i is the $N_r \times N_r$ amplifying matrix at the i th relay node. The received signal vector at the destination node can be written as

$$\mathbf{y}_d = \sum_{i=1}^K \mathbf{H}_{rd,i} \mathbf{x}_{r,i} + \mathbf{v}_d \quad (3.4)$$

where $\mathbf{H}_{rd,i}$ is the $N_d \times N_r$ MIMO channel matrix between the i th relay and the destination nodes, \mathbf{v}_d is the additive Gaussian noise vector at the destination node. Substituting (3.1)-(3.3) into (3.4), we have

$$\begin{aligned} \mathbf{y}_d &= \sum_{i=1}^K (\mathbf{H}_{rd,i} \mathbf{F}_i \mathbf{H}_{sr,i} \mathbf{B} \mathbf{s} + \mathbf{H}_{rd,i} \mathbf{F}_i \mathbf{v}_{r,i}) + \mathbf{v}_d \\ &= \mathbf{H}_{rd} \mathbf{F} \mathbf{H}_{sr} \mathbf{B} \mathbf{s} + \mathbf{H}_{rd} \mathbf{F} \mathbf{v}_r + \mathbf{v}_d \\ &\triangleq \bar{\mathbf{H}} \mathbf{s} + \bar{\mathbf{v}} \end{aligned} \quad (3.5)$$

where $\mathbf{H}_{sr} \triangleq [\mathbf{H}_{sr,1}^T, \mathbf{H}_{sr,2}^T, \dots, \mathbf{H}_{sr,K}^T]^T$ is a $KN_r \times N_s$ channel matrix between the source node and all relay nodes, $\mathbf{H}_{rd} \triangleq [\mathbf{H}_{rd,1}, \mathbf{H}_{rd,2}, \dots, \mathbf{H}_{rd,K}]$ is an $N_d \times KN_r$ channel matrix between all relay nodes and the destination node, $\mathbf{F} \triangleq \text{bd}[\mathbf{F}_1, \mathbf{F}_2, \dots, \mathbf{F}_K]$ is the $KN_r \times KN_r$ block diagonal equivalent relay matrix, $\mathbf{v}_r \triangleq [\mathbf{v}_{r,1}^T, \mathbf{v}_{r,2}^T, \dots, \mathbf{v}_{r,K}^T]^T$ is obtained by stacking the noise vectors at all the relays, $\bar{\mathbf{H}} \triangleq \mathbf{H}_{rd} \mathbf{F} \mathbf{H}_{sr} \mathbf{B}$ is the effective MIMO channel matrix of the source-relay-destination link, and $\bar{\mathbf{v}} \triangleq \mathbf{H}_{rd} \mathbf{F} \mathbf{v}_r + \mathbf{v}_d$ is the equivalent noise vector. We assume that all noises are i.i.d. Gaussian noise with zero mean and unit variance. The diagram of the equivalent MIMO relay system with multiple data streams described by (3.5) is shown in Fig. 3.2. The transmission power consumed by each relay node (3.3) can be expressed as

$$\mathbb{E}[\text{tr}(\mathbf{x}_{r,i} \mathbf{x}_{r,i}^H)] = \text{tr}(\mathbf{F}_i [\mathbf{H}_{sr,i} \mathbf{B} \mathbf{B}^H \mathbf{H}_{sr,i}^H + \mathbf{I}_{N_r}] \mathbf{F}_i^H), \quad i = 1, \dots, K. \quad (3.6)$$

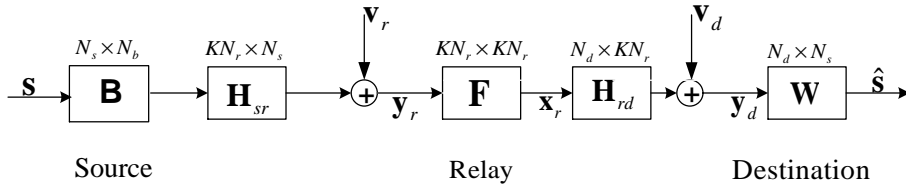


Figure 3.2: Block diagram of the equivalent MIMO relay system with multiple data streams.

By using a linear receiver, the estimated signal waveform vector at the destination node is given by $\hat{\mathbf{s}} = \mathbf{W}^H \mathbf{y}_d$, where \mathbf{W} is an $N_d \times N_b$ weight matrix. The MSE of the

signal waveform estimation is given by

$$\begin{aligned} \text{MSE} &= \text{tr}\left(\mathbb{E}\left[(\hat{\mathbf{s}} - \mathbf{s})(\hat{\mathbf{s}} - \mathbf{s})^H\right]\right) \\ &= \text{tr}\left((\mathbf{W}^H \bar{\mathbf{H}} - \mathbf{I}_{N_b})(\mathbf{W}^H \bar{\mathbf{H}} - \mathbf{I}_{N_b})^H + \mathbf{W}^H \mathbf{C}_{\bar{v}} \mathbf{W}\right). \end{aligned} \quad (3.7)$$

The weight matrix \mathbf{W} which minimizes (3.7) is the Wiener filter and can be written as

$$\mathbf{W} = (\bar{\mathbf{H}}\bar{\mathbf{H}}^H + \mathbf{C}_{\bar{v}})^{-1}\bar{\mathbf{H}}. \quad (3.8)$$

Substituting (3.8) back into (3.7), it can be seen that the MSE is a function of \mathbf{F} and \mathbf{B} and can be written as

$$\text{MSE} = \text{tr}\left([\mathbf{I}_{N_b} + \bar{\mathbf{H}}^H \mathbf{C}_{\bar{v}}^{-1} \bar{\mathbf{H}}]^{-1}\right). \quad (3.9)$$

3.3 Joint Source and Relay Matrices Optimization

In this section, we address the joint source and relay matrices optimization problem for MIMO multi-relay systems with a linear MMSE receiver at the destination node. In particular, we show that optimal relay matrices have a general beamforming structure. Based on (3.6) and (3.9), the joint source and relay matrices optimization problem can be formulated as

$$\min_{\{\mathbf{F}_i\}, \mathbf{B}} \text{tr}\left([\mathbf{I}_{N_b} + \bar{\mathbf{H}}^H \mathbf{C}_{\bar{v}}^{-1} \bar{\mathbf{H}}]^{-1}\right) \quad (3.10)$$

$$\text{s.t.} \quad \text{tr}(\mathbf{B}\mathbf{B}^H) \leq P_s \quad (3.11)$$

$$\text{tr}(\mathbf{F}_i [\mathbf{H}_{sr,i} \mathbf{B} \mathbf{B}^H \mathbf{H}_{sr,i}^H + \mathbf{I}_{N_r}] \mathbf{F}_i^H) \leq P_{r,i}, \quad i = 1, \dots, K \quad (3.12)$$

where $\{\mathbf{F}_i\} \triangleq \{\mathbf{F}_i, i = 1, \dots, L\}$, (3.11) is the transmit power constraint at the source node, while (3.12) is the power constraint at each relay node. Here $P_s > 0$ and $P_{r,i} > 0$, $i = 1, \dots, K$, are the corresponding power budget. Obviously, to avoid any loss of transmission power in the relay system when a linear receiver is used, there should be $N_b \leq \min(N_s, KN_r, N_d)$. The problem (3.10)-(3.12) is nonconvex and a globally optimal solution of \mathbf{B} and $\{\mathbf{F}_i\}$ is difficult to obtain with a reasonable computational complexity. In the following, we develop an iterative algorithm to optimize \mathbf{B} and $\{\mathbf{F}_i\}$. First we show the optimal structure of $\{\mathbf{F}_i\}$.

3.3.1 Optimal Structure of Relay Amplifying Matrices

For given source matrix \mathbf{B} satisfying (3.11), the relay matrices $\{\mathbf{F}_i\}$ are optimized by solving the following problem

$$\min_{\{\mathbf{F}_i\}} \quad \text{tr} \left([\mathbf{I}_{N_b} + \bar{\mathbf{H}}^H \mathbf{C}_{\bar{v}}^{-1} \bar{\mathbf{H}}]^{-1} \right) \quad (3.13)$$

$$\text{s.t.} \quad \text{tr}(\mathbf{F}_i [\mathbf{H}_{sr,i} \mathbf{B} \mathbf{B}^H \mathbf{H}_{sr,i}^H + \mathbf{I}_{N_r}] \mathbf{F}_i^H) \leq P_{r,i}, \quad i = 1, \dots, K. \quad (3.14)$$

Let us introduce the following singular value decompositions (SVDs)

$$\mathbf{H}_{sr,i} \mathbf{B} = \mathbf{U}_{s,i} \boldsymbol{\Lambda}_{s,i} \mathbf{V}_{s,i}^H, \quad \mathbf{H}_{rd,i} = \mathbf{U}_{r,i} \boldsymbol{\Lambda}_{r,i} \mathbf{V}_{r,i}^H, \quad i = 1, \dots, K \quad (3.15)$$

where $\boldsymbol{\Lambda}_{s,i}$ and $\boldsymbol{\Lambda}_{r,i}$ are $R_{s,i} \times R_{s,i}$ and $R_{r,i} \times R_{r,i}$ diagonal matrices, respectively. Here $R_{s,i} \triangleq \text{rank}(\mathbf{H}_{sr,i} \mathbf{B})$, $R_{r,i} \triangleq \text{rank}(\mathbf{H}_{rd,i})$, $i = 1, \dots, K$. Based on the definition of matrix rank, $R_{s,i} \leq \min(N_r, N_b)$ and $R_{r,i} \leq \min(N_r, N_d)$. The following theorem states the structure of the optimal $\{\mathbf{F}_i\}$.

THEOREM 3.1: By using the SVDs of (3.15), the optimal structure of \mathbf{F}_i as the solution to the problem (3.13)-(3.14) is given by

$$\mathbf{F}_i = \mathbf{V}_{r,i} \mathbf{A}_i \mathbf{U}_{s,i}^H, \quad i = 1, \dots, K \quad (3.16)$$

where \mathbf{A}_i is an $R_{r,i} \times R_{s,i}$ matrix, $i = 1, \dots, K$.

PROOF: See Appendix 3.A. □

The remaining task is to find the optimal \mathbf{A}_i , $i = 1, \dots, K$. From (3.31) and (3.32), we can equivalently rewrite the optimization problem (3.13)-(3.14) as

$$\min_{\{\mathbf{A}_i\}} \quad \text{tr} \left(\left[\mathbf{I}_{N_b} + \sum_{i=1}^K \mathbf{V}_{s,i} \boldsymbol{\Lambda}_{s,i} \mathbf{A}_i^H \boldsymbol{\Lambda}_{r,i} \mathbf{U}_{r,i}^H \left(\sum_{i=1}^K \mathbf{U}_{r,i} \boldsymbol{\Lambda}_{r,i} \mathbf{A}_i \mathbf{A}_i^H \boldsymbol{\Lambda}_{r,i} \mathbf{U}_{r,i}^H + \mathbf{I}_{N_d} \right)^{-1} \right. \right. \\ \left. \left. \times \sum_{i=1}^K \mathbf{U}_{r,i} \boldsymbol{\Lambda}_{r,i} \mathbf{A}_i \boldsymbol{\Lambda}_{s,i} \mathbf{V}_{s,i}^H \right]^{-1} \right) \quad (3.17)$$

$$\text{s.t.} \quad \text{tr}(\mathbf{A}_i (\boldsymbol{\Lambda}_{s,i}^2 + \mathbf{I}_{R_{s,i}}) \mathbf{A}_i^H) \leq P_{r,i}, \quad i = 1, \dots, K. \quad (3.18)$$

Both the problem (3.13)-(3.14) and the problem (3.17)-(3.18) have matrix optimization variables. However, in the former problem, the optimization variable \mathbf{F}_i is an $N_r \times N_r$ matrix, while the dimension of \mathbf{A}_i is $R_{r,i} \times R_{s,i}$, which may be smaller than that of \mathbf{F}_i . Thus, solving the problem (3.17)-(3.18) has a smaller computational complexity than solving the problem (3.13)-(3.14). In general, the problem (3.17)-(3.18) is nonconvex and a globally optimal solution is difficult to obtain with a reasonable computational

complexity. Fortunately, we can resort to numerical method, such as the projected gradient algorithm [107] to find (at least) a locally optimal solution of (3.17)-(3.18).

THEOREM 3.2: Let us define the objective function in (3.17) as $f(\mathbf{A}_i)$. Its gradient $\nabla f(\mathbf{A}_i)$ with respect to \mathbf{A}_i can be calculated by using results on derivatives of matrices in [108] as

$$\nabla f(\mathbf{A}_i) = 2(\mathbf{R}_i^H \mathbf{M}_i^H (\mathbf{E}_i \mathbf{S}_i^H + \mathbf{D}_i^H) - \mathbf{R}_i^H \mathbf{G}_i^{-H} \mathbf{E}_i \mathbf{S}_i^H), \quad i = 1, \dots, K \quad (3.19)$$

where $\mathbf{M}_i, \mathbf{R}_i, \mathbf{S}_i, \mathbf{D}_i, \mathbf{E}_i$, and \mathbf{G}_i are defined in Appendix 3.B.

PROOF: See Appendix 3.B. \square

In each iteration of the PG algorithm, we first obtain $\tilde{\mathbf{A}}_i = \mathbf{A}_i - s_n \nabla f(\mathbf{A}_i)$ by moving \mathbf{A}_i one step towards the negative gradient direction of $f(\mathbf{A}_i)$, where $s_n > 0$ is the step size. Since $\tilde{\mathbf{A}}_i$ might not satisfy the constraint (3.18), we need to project it onto the set given by (3.18). The projected matrix $\bar{\mathbf{A}}_i$ is obtained by minimizing the Frobenius norm of $\bar{\mathbf{A}}_i - \tilde{\mathbf{A}}_i$ (according to [107]) subjecting to (3.18), which can be formulated as the following optimization problem

$$\min_{\bar{\mathbf{A}}_i} \quad \text{tr}((\bar{\mathbf{A}}_i - \tilde{\mathbf{A}}_i)(\bar{\mathbf{A}}_i - \tilde{\mathbf{A}}_i)^H) \quad (3.20)$$

$$\text{s.t.} \quad \text{tr}(\bar{\mathbf{A}}_i(\boldsymbol{\Lambda}_{s,i}^2 + \mathbf{I}_{R_{s,i}})\bar{\mathbf{A}}_i^H) \leq P_{r,i}. \quad (3.21)$$

Obviously, if $\text{tr}(\tilde{\mathbf{A}}_i(\boldsymbol{\Lambda}_{s,i}^2 + \mathbf{I}_{R_{s,i}})\tilde{\mathbf{A}}_i^H) \leq P_{r,i}$, then $\bar{\mathbf{A}}_i = \tilde{\mathbf{A}}_i$. Otherwise, the solution to the problem (3.20)-(3.21) can be obtained by using the Lagrange multiplier method, and the solution is given by

$$\bar{\mathbf{A}}_i = \tilde{\mathbf{A}}_i [(\lambda + 1)\mathbf{I}_{R_{s,i}} + \lambda \boldsymbol{\Lambda}_{s,i}^2]^{-1}$$

where $\lambda > 0$ is the solution to the nonlinear equation of

$$\text{tr}(\tilde{\mathbf{A}}_i [(\lambda + 1)\mathbf{I}_{R_{s,i}} + \lambda \boldsymbol{\Lambda}_{s,i}^2]^{-1} (\boldsymbol{\Lambda}_{s,i}^2 + \mathbf{I}_{R_{s,i}}) [(\lambda + 1)\mathbf{I}_{R_{s,i}} + \lambda \boldsymbol{\Lambda}_{s,i}^2]^{-1} \tilde{\mathbf{A}}_i^H) = P_{r,i}. \quad (3.22)$$

Equation (3.22) can be efficiently solved by the bisection method [107].

The procedure of the PG algorithm is listed in Table 3.1. δ_n and s_n are the step size parameters at the n th iteration, and ε is a positive constant close to 0. The step size parameters δ_n and s_n are determined by the Armijo rule [107], i.e., $s_n = s$ is a constant through all iterations, while at the n th iteration, δ_n is set to be γ^{m_n} . Here m_n is the minimal nonnegative integer that satisfies the following inequality $f(\mathbf{A}_i^{(n+1)}) - f(\mathbf{A}_i^{(n)}) \leq \alpha \gamma^{m_n} \text{tr}((\nabla f(\mathbf{A}_i^{(n)}))^H (\bar{\mathbf{A}}_i^{(n)} - \mathbf{A}_i^{(n)}))$, where α and γ are constants. According to [107], usually α is chosen close to 0, for example $\alpha \in [10^{-5}, 10^{-1}]$, while a proper choice of γ is normally from 0.1 to 0.5.

Table 3.1: Procedure of applying the projected gradient algorithm to solve the problem (3.17)-(3.18)

1. Initialize the algorithm at a feasible $\mathbf{A}_i^{(0)}$ for $i = 1, \dots, K$; Set $n = 0$.
2. For $i = 1, \dots, K$,
 - Compute the gradient of (3.17) $\nabla f(\mathbf{A}_i^{(n)})$;
 - Project $\tilde{\mathbf{A}}_i^{(n)} = \mathbf{A}_i^{(n)} - s_n \nabla f(\mathbf{A}_i^{(n)})$ to obtain $\bar{\mathbf{A}}_i^{(n)}$;
 - Update \mathbf{A}_i with $\mathbf{A}_i^{(n+1)} = \mathbf{A}_i^{(n)} + \delta_n (\bar{\mathbf{A}}_i^{(n)} - \mathbf{A}_i^{(n)})$.
3. If $\max_i \|\mathbf{A}_i^{(n+1)} - \mathbf{A}_i^{(n)}\| \leq \varepsilon$, then end.
 Otherwise, let $n := n + 1$ and go to step 2).

3.3.2 Optimal Source Precoding Matrix

With fixed $\{\mathbf{F}_i\}$, the source precoding matrix \mathbf{B} is optimized by solving the following problem

$$\min_{\mathbf{B}} \quad \text{tr} \left([\mathbf{I}_{N_b} + \mathbf{B}^H \boldsymbol{\Psi} \mathbf{B}]^{-1} \right) \quad (3.23)$$

$$\text{s.t.} \quad \text{tr}(\mathbf{B} \mathbf{B}^H) \leq P_s, \quad (3.24)$$

$$\text{tr}(\mathbf{F}_i \mathbf{H}_{sr,i} \mathbf{B} \mathbf{B}^H \mathbf{H}_{sr,i}^H \mathbf{F}_i^H) \leq \bar{P}_{r,i}, \quad i = 1, \dots, K \quad (3.25)$$

where $\boldsymbol{\Psi} \triangleq \mathbf{H}_{sr}^H \mathbf{F}^H \mathbf{H}_{rd}^H (\mathbf{H}_{rd} \mathbf{F} \mathbf{F}^H \mathbf{H}_{rd}^H + \mathbf{I}_{N_d})^{-1} \mathbf{H}_{rd} \mathbf{F} \mathbf{H}_{sr}$, and $\bar{P}_{r,i} \triangleq P_{r,i} - \text{tr}(\mathbf{F}_i \mathbf{F}_i^H)$, $i = 1, \dots, K$. Let us introduce $\boldsymbol{\Omega} \triangleq \mathbf{B} \mathbf{B}^H$, and a positive semi-definite (PSD) matrix \mathbf{X} with $\mathbf{X} \succeq (\mathbf{I}_{N_s} + \boldsymbol{\Psi}^{\frac{1}{2}} \boldsymbol{\Omega} \boldsymbol{\Psi}^{\frac{1}{2}})^{-1}$, where $\mathbf{A} \succeq \mathbf{B}$ means that $\mathbf{A} - \mathbf{B}$ is a PSD matrix. By using the Schur complement [106], the problem (3.23)-(3.25) can be equivalently converted to the following problem

$$\min_{\mathbf{X}, \boldsymbol{\Omega}} \quad \text{tr}(\mathbf{X}) \quad (3.26)$$

$$\text{s.t.} \quad \begin{pmatrix} \mathbf{X} & \mathbf{I}_{N_s} \\ \mathbf{I}_{N_s} & \mathbf{I}_{N_s} + \boldsymbol{\Psi}^{\frac{1}{2}} \boldsymbol{\Omega} \boldsymbol{\Psi}^{\frac{1}{2}} \end{pmatrix} \succeq 0, \quad (3.27)$$

$$\text{tr}(\boldsymbol{\Omega}) \leq P_s, \quad \boldsymbol{\Omega} \succeq 0, \quad (3.28)$$

$$\text{tr}(\mathbf{F}_i \mathbf{H}_{sr,i} \boldsymbol{\Omega} \mathbf{H}_{sr,i}^H \mathbf{F}_i^H) \leq \bar{P}_{r,i}, \quad i = 1, \dots, K. \quad (3.29)$$

The problem (3.26)-(3.29) is a convex semi-definite programming (SDP) problem which can be efficiently solved by the interior-point method [106]. Let us introduce the

eigenvalue decomposition (EVD) of $\mathbf{\Omega} = \mathbf{U}_\Omega \mathbf{\Lambda}_\Omega \mathbf{U}_\Omega^H$. Then from $\mathbf{\Omega} = \mathbf{B}\mathbf{B}^H$, we have $\mathbf{B} = \mathbf{U}_\Omega \mathbf{\Lambda}_\Omega^{\frac{1}{2}}$.

Table 3.2: Procedure of solving the problem (3.10)-(3.12).

1. Initialize the algorithm at a feasible $\mathbf{B}^{(0)}$ satisfying constraint (3.11); Set $m = 0$.
2. For fixed $\mathbf{B}^{(m)}$, obtain $\{\mathbf{F}_i\}^{(m)}$ by solving the problem (3.17)-(3.18) using the PG algorithm.
3. Update $\mathbf{B}^{(m+1)}$ by solving the problem (3.26)-(3.29) with known $\{\mathbf{F}_i\}^{(m)}$.
4. If $\|\mathbf{B}^{(m+1)} - \mathbf{B}^{(m)}\| \leq \varepsilon$, then end.
Otherwise, let $m := m + 1$ and go to step 2).

Now the original joint source and relay optimization problem (3.10)-(3.12) can be solved by an iterative algorithm as shown in Table 3.2. This algorithm is first initialized at a random feasible \mathbf{B} satisfying (3.11). At each iteration, we first update $\{\mathbf{F}_i\}$ with fixed \mathbf{B} and then update \mathbf{B} with fixed $\{\mathbf{F}_i\}$. Note that the conditional updates of each matrix may either decrease or maintain but cannot increase the objective function (3.10). Monotonic convergence of $\{\mathbf{F}_i\}$ and \mathbf{B} towards (at least) a locally optimal solution follows directly from this observation.

3.4 Numerical Examples

In this section, we study the performance of the proposed the optimal source precoding matrix and relay amplifying matrices for two-hop non-regenerative MIMO multi-relay systems with multiple data streams when a linear MMSE receiver is used at the destination node. All simulations are conducted in a flat Rayleigh fading environment where the channel matrices have zero-mean entries with variances σ_s^2/N_s and $\sigma_r^2/(KN_r)$ for \mathbf{H}_{sr} and \mathbf{H}_{rd} , respectively. The BPSK constellations are used to modulate the source symbols, and all noises are i.i.d. Gaussian with zero mean and unit variance. We define $\text{SNR}_s = \sigma_s^2 P_s KN_r / N_s$ and $\text{SNR}_r = \sigma_r^2 P_r N_d / (KN_r)$ as the SNR for the source-relay link (SNR_s) and the relay-destination link (SNR_r), respectively. We transmit 1000 randomly generated bits in each channel realization, and all simulation results are averaged

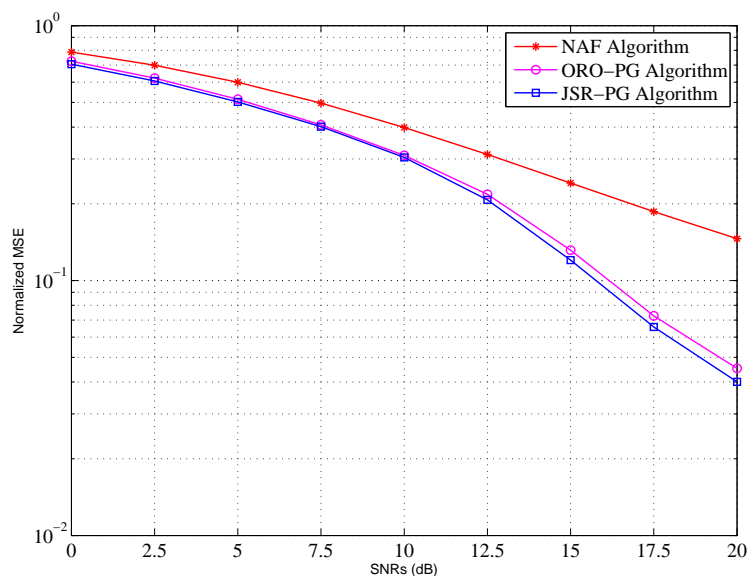


Figure 3.3: Example 3.1 Normalized MSE versus SNR_s with $K = 3$.

over 200 channel realizations. In all simulations, the linear MMSE receiver in (3.8) is employed at destination node for symbol detection.

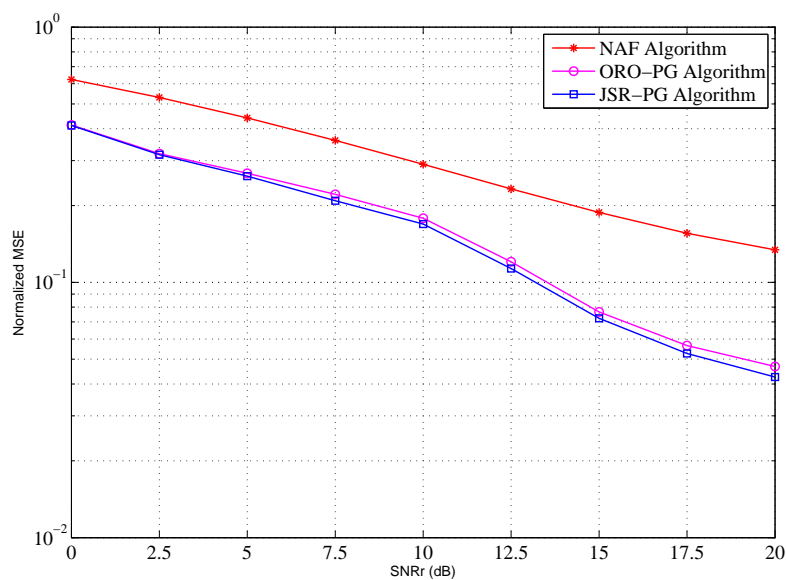


Figure 3.4: Example 3.1 Normalized MSE versus SNR_r with $K = 3$.

In the first example, a MIMO multi-relay communication system with $K = 3$ re-

lay nodes and $N_s = N_r = N_d = 3$ is simulated. We compare the normalized MSE performance of the proposed joint source and relay optimization algorithm using the projected gradient (JSR-PG) algorithm in Table 3.2, the optimal relay-only algorithm using the projected gradient (ORO-PG) algorithm in Table 3.1, and the naive amplify-and-forward (NAF) algorithm where both the source and relay matrices are scaled identity matrices. Fig. 3.3 shows the normalized MSE of all algorithms versus SNR_s for $\text{SNR}_r = 20\text{dB}$. While Fig. 3.4 demonstrates the normalized MSE of all algorithms versus SNR_r for SNR_s fixed at 20dB. It can be seen from Figs. 3.3 and 3.4 that the JSR-PG and ORO-PG algorithms have a better performance than the NAF algorithm over the whole SNR_s and SNR_r range. Moreover, the proposed JSR-PG algorithm yields the lowest MSE among all three algorithms.

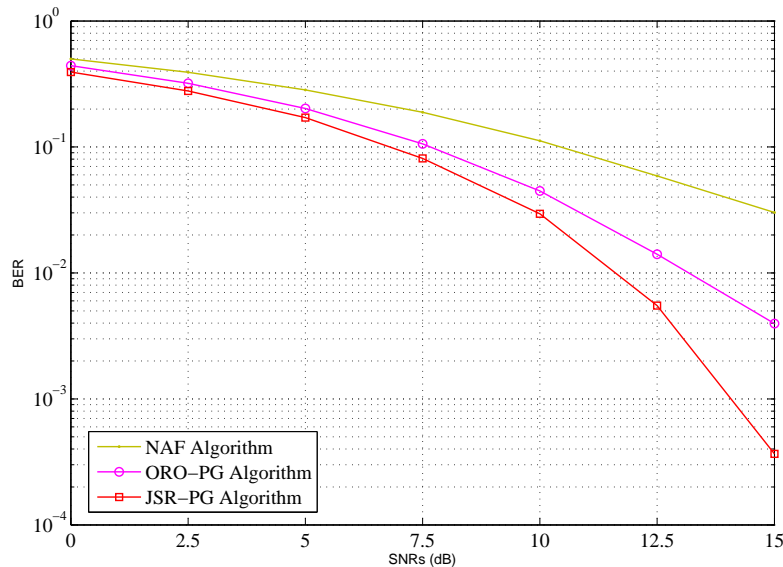


Figure 3.5: Example 3.2 BER versus SNR_s with $K = 3$.

In the second example, we compare the BER performance of the proposed JSR-PG algorithm in Table 3.2, the ORO-PG algorithm in Table 3.1, and the NAF algorithm. Fig. 3.5 displays the system BER versus SNR_s for a MIMO multi-relay communication system with $K = 3$ relay nodes, $N_s = N_r = N_d = 3$, and SNR_r fixed at 20dB. It can be seen from Fig. 3.5 that the proposed JSR-PG algorithm has a better BER performance than existing algorithms over the whole SNR_s range.

In the third example, we study the effect of the number of relay nodes to the system BER performance using the JSR-PG and ORO-PG algorithms. Fig. 3.6 displays the

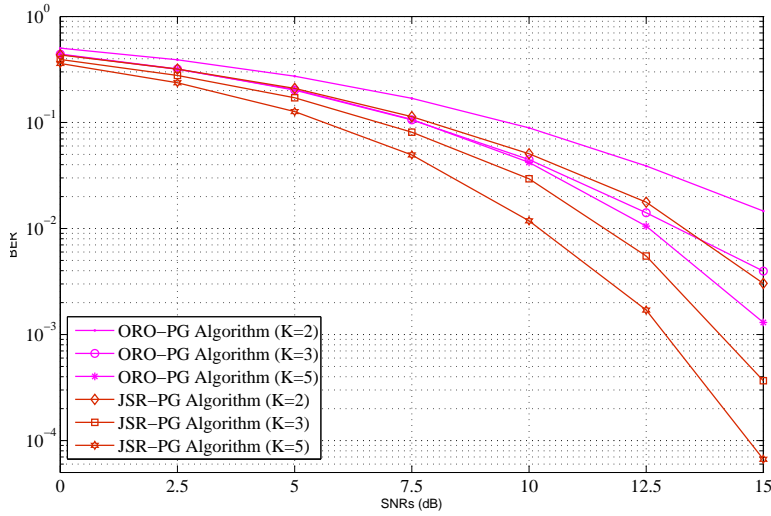


Figure 3.6: Example 3.3 BER versus SNR_s with different K .

system BER versus SNR_s with $K = 2, 3$, and 5 for SNR_r fixed at 20dB and $N_s = N_r = N_d = 3$. It can be seen that at $\text{BER} = 10^{-2}$, for both the ORO-PG algorithm and JSR-PG algorithm, we can achieve approximately 3dB gain by increasing from $K = 2$ to $K = 5$. It can also be seen that the performance gain of the JSR-PG algorithm over the ORO-PG algorithm increases with the increasing number of relay nodes.

3.5 Chapter Summary

In this chapter, we have derived the general structure of the optimal relay amplifying matrices for a linear non-regenerative MIMO relay system where each relay has multiple antennas and multiple data streams are transmitted from the source to the destination node. The proposed source and relay matrices minimize the MSE of the signal waveform estimation when a linear receiver is used at the destination node. Simulation results demonstrate the effectiveness of the proposed source and relay matrices design using the projected gradient (PG) approach.

3.A Proof of Theorem 3.1.

Without loss of generality, \mathbf{F}_i can be written as

$$\mathbf{F}_i = \begin{bmatrix} \mathbf{V}_{r,i} & \mathbf{V}_{r,i}^\perp \end{bmatrix} \begin{bmatrix} \mathbf{A}_i & \mathbf{X}_i \\ \mathbf{Y}_i & \mathbf{Z}_i \end{bmatrix} \begin{bmatrix} \mathbf{U}_{s,i}^H \\ (\mathbf{U}_{s,i}^\perp)^H \end{bmatrix}, \quad i = 1, \dots, K \quad (3.30)$$

where $\mathbf{V}_{r,i}^\perp (\mathbf{V}_{r,i}^\perp)^H = \mathbf{I}_{N_r} - \mathbf{V}_{r,i} \mathbf{V}_{r,i}^H$, $\mathbf{U}_{s,i}^\perp (\mathbf{U}_{s,i}^\perp)^H = \mathbf{I}_{N_r} - \mathbf{U}_{s,i} \mathbf{U}_{s,i}^H$, such that $\bar{\mathbf{V}}_{r,i} \triangleq [\mathbf{V}_{r,i}, \mathbf{V}_{r,i}^\perp]$ and $\bar{\mathbf{U}}_{s,i} \triangleq [\mathbf{U}_{s,i}, \mathbf{U}_{s,i}^\perp]$ are $N_r \times N_r$ unitary matrices. Matrices $\mathbf{A}_i, \mathbf{X}_i, \mathbf{Y}_i, \mathbf{Z}_i$ are arbitrary matrices with dimensions of $R_{r,i} \times R_{s,i}$, $R_{r,i} \times (N_r - R_{s,i})$, $(N_r - R_{r,i}) \times R_{s,i}$, $(N_r - R_{r,i}) \times (N_r - R_{s,i})$, respectively. Substituting (3.15) and (3.30) back into (3.13), we obtain that $\mathbf{H}_{rd,i} \mathbf{F}_i \mathbf{H}_{sr,i} \mathbf{B} = \mathbf{U}_{r,i} \mathbf{\Lambda}_{r,i} \mathbf{A}_i \mathbf{\Lambda}_{s,i} \mathbf{V}_{s,i}^H$ and $\mathbf{H}_{rd,i} \mathbf{F}_i \mathbf{F}_i^H \mathbf{H}_{rd,i}^H = \mathbf{U}_{r,i} \mathbf{\Lambda}_{r,i} (\mathbf{A}_i \mathbf{A}_i^H + \mathbf{X}_i \mathbf{X}_i^H) \mathbf{\Lambda}_{r,i}^H \mathbf{U}_{r,i}^H$. Thus we can rewrite (3.13) as

$$\begin{aligned} \text{MSE} = & \text{tr} \left(\left[\mathbf{I}_{N_b} + \sum_{i=1}^K \mathbf{V}_{s,i} \mathbf{\Lambda}_{s,i} \mathbf{A}_i^H \mathbf{\Lambda}_{r,i} \mathbf{U}_{r,i}^H \left(\sum_{i=1}^K \mathbf{U}_{r,i} \mathbf{\Lambda}_{r,i} (\mathbf{A}_i \mathbf{A}_i^H + \mathbf{X}_i \mathbf{X}_i^H) \mathbf{\Lambda}_{r,i}^H \mathbf{U}_{r,i}^H + \mathbf{I}_{N_d} \right) \right. \right. \\ & \left. \left. \times \sum_{i=1}^K \mathbf{U}_{r,i} \mathbf{\Lambda}_{r,i} \mathbf{A}_i \mathbf{\Lambda}_{s,i} \mathbf{V}_{s,i}^H \right]^{-1} \right). \end{aligned} \quad (3.31)$$

It can be seen that (3.31) is minimized by $\mathbf{X}_i = \mathbf{0}_{R_{r,i} \times (N_r - R_{s,i})}$, $i = 1, \dots, K$.

Substituting (3.15) and (3.30) back into the left-hand-side of the transmission power constraint (3.14), we have

$$\begin{aligned} & \text{tr} (\mathbf{F}_i [\mathbf{H}_{sr,i} \mathbf{B} \mathbf{B}^H \mathbf{H}_{sr,i}^H + \mathbf{I}_{N_r}] \mathbf{F}_i^H) \\ & = \text{tr} (\mathbf{A}_i (\mathbf{\Lambda}_{s,i}^2 + \mathbf{I}_{R_{s,i}}) \mathbf{A}_i^H + \mathbf{Y}_i (\mathbf{\Lambda}_{s,i}^2 + \mathbf{I}_{R_{s,i}}) \mathbf{Y}_i^H + \mathbf{X}_i \mathbf{X}_i^H + \mathbf{Z}_i \mathbf{Z}_i^H), \quad i = 1, \dots, K. \end{aligned} \quad (3.32)$$

From (3.32), we find that $\mathbf{X}_i = \mathbf{0}_{R_{r,i} \times (N_r - R_{s,i})}$, $\mathbf{Y}_i = \mathbf{0}_{(N_r - R_{r,i}) \times R_{s,i}}$, and

$\mathbf{Z}_i = \mathbf{0}_{(N_r - R_{r,i}) \times (N_r - R_{s,i})}$ minimize the power consumption at each relay node. Thus we have $\mathbf{F}_i = \mathbf{V}_{r,i} \mathbf{A}_i \mathbf{U}_{s,i}^H$, $i = 1, \dots, K$.

3.B Proof of Theorem 3.2.

Let us define $\mathbf{Z}_i \triangleq \sum_{j=1, j \neq i}^K \mathbf{U}_{r,j} \mathbf{\Lambda}_{r,j} \mathbf{A}_j \mathbf{\Lambda}_{s,j} \mathbf{V}_{s,j}^H$ and

$\mathbf{Y}_i \triangleq \sum_{j=1, j \neq i}^K \mathbf{U}_{r,j} \mathbf{\Lambda}_{r,j} \mathbf{A}_j \mathbf{A}_j^H \mathbf{\Lambda}_{r,j} \mathbf{U}_{r,j}^H + \mathbf{I}_{N_d}$. Then $f(\mathbf{A}_i)$ can be written as

$$\begin{aligned} f(\mathbf{A}_i) = & \text{tr} \left(\left[\mathbf{I}_{N_b} + (\mathbf{Z}_i^H + \mathbf{V}_{s,i} \mathbf{\Lambda}_{s,i} \mathbf{A}_i^H \mathbf{\Lambda}_{r,i} \mathbf{U}_{r,i}^H) (\mathbf{Y}_i + \mathbf{U}_{r,i} \mathbf{\Lambda}_{r,i} \mathbf{A}_i \mathbf{A}_i^H \mathbf{\Lambda}_{r,i} \mathbf{U}_{r,i}^H) \right. \right. \\ & \left. \left. \times (\mathbf{Z}_i + \mathbf{U}_{r,i} \mathbf{\Lambda}_{r,i} \mathbf{A}_i \mathbf{\Lambda}_{s,i} \mathbf{V}_{s,i}^H) \right]^{-1} \right). \end{aligned} \quad (3.33)$$

Applying $(\mathbf{I}_{N_b} + \mathbf{A}^H \mathbf{C}^{-1} \mathbf{A})^{-1} = \mathbf{I}_{N_b} - \mathbf{A}^H (\mathbf{A} \mathbf{A}^H + \mathbf{C})^{-1} \mathbf{A}$, (3.33) can be written as

$$\begin{aligned} f(\mathbf{A}_i) &= \text{tr}(\mathbf{I}_{N_b} - (\mathbf{Z}_i^H + \mathbf{V}_{s,i} \boldsymbol{\Lambda}_{s,i} \mathbf{A}_i^H \boldsymbol{\Lambda}_{r,i} \mathbf{U}_{r,i}^H) [(\mathbf{Z}_i + \mathbf{U}_{r,i} \boldsymbol{\Lambda}_{r,i} \mathbf{A}_i \boldsymbol{\Lambda}_{s,i} \mathbf{V}_{s,i}^H) \\ &\quad \times (\mathbf{Z}_i^H + \mathbf{V}_{s,i} \boldsymbol{\Lambda}_{s,i} \mathbf{A}_i^H \boldsymbol{\Lambda}_{r,i} \mathbf{U}_{r,i}^H) + \mathbf{Y}_i + \mathbf{U}_{r,i} \boldsymbol{\Lambda}_{r,i} \mathbf{A}_i \mathbf{A}_i^H \boldsymbol{\Lambda}_{r,i} \mathbf{U}_{r,i}^H]^{-1} \\ &\quad (\mathbf{Z}_i + \mathbf{U}_{r,i} \boldsymbol{\Lambda}_{r,i} \mathbf{A}_i \boldsymbol{\Lambda}_{s,i} \mathbf{V}_{s,i}^H)). \end{aligned} \quad (3.34)$$

Let us now define $\mathbf{E}_i \triangleq \mathbf{Z}_i + \mathbf{U}_{r,i} \boldsymbol{\Lambda}_{r,i} \mathbf{A}_i \boldsymbol{\Lambda}_{s,i} \mathbf{V}_{s,i}^H$, $\mathbf{K}_i \triangleq \mathbf{Y}_i + \mathbf{U}_{r,i} \boldsymbol{\Lambda}_{r,i} \mathbf{A}_i \mathbf{A}_i^H \boldsymbol{\Lambda}_{r,i} \mathbf{U}_{r,i}^H$, and $\mathbf{G}_i \triangleq \mathbf{E}_i \mathbf{E}_i^H + \mathbf{K}_i$. We can rewrite (3.34) as

$$f(\mathbf{A}_i) = \text{tr}(\mathbf{I}_{N_b} - \mathbf{E}_i^H \mathbf{G}_i^{-1} \mathbf{E}_i) = \text{tr}(\mathbf{I}_{N_b} - \mathbf{E}_i \mathbf{E}_i^H \mathbf{G}_i^{-1}). \quad (3.35)$$

The derivative of $f(\mathbf{A}_i)$ with respect to \mathbf{A}_i is given by

$$\begin{aligned} \frac{\partial f(\mathbf{A}_i)}{\partial \mathbf{A}_i} &= -\frac{\partial}{\partial \mathbf{A}_i} \text{tr}(\mathbf{E}_i \mathbf{E}_i^H \mathbf{G}_i^{-1}) \\ &= \frac{\partial}{\partial \mathbf{A}_i} \text{tr}(\mathbf{G}_i^{-1} \mathbf{E}_i \mathbf{E}_i^H \mathbf{G}_i^{-1} ((\mathbf{Z}_i + \mathbf{U}_{r,i} \boldsymbol{\Lambda}_{r,i} \mathbf{A}_i \boldsymbol{\Lambda}_{s,i} \mathbf{V}_{s,i}^H) \mathbf{E}_i^H \\ &\quad + \mathbf{Y}_i + \mathbf{U}_{r,i} \boldsymbol{\Lambda}_{r,i} \mathbf{A}_i \mathbf{A}_i^H \boldsymbol{\Lambda}_{r,i} \mathbf{U}_{r,i}^H)) - \frac{\partial}{\partial \mathbf{A}_i} \text{tr}(\mathbf{E}_i^H \mathbf{G}_i^{-1} \mathbf{U}_{r,i} \boldsymbol{\Lambda}_{r,i} \mathbf{A}_i \boldsymbol{\Lambda}_{s,i} \mathbf{V}_{s,i}^H). \end{aligned} \quad (3.36)$$

Defining $\mathbf{M}_i \triangleq \mathbf{G}_i^{-1} \mathbf{E}_i \mathbf{E}_i^H \mathbf{G}_i^{-1}$, $\mathbf{R}_i \triangleq \mathbf{U}_{r,i} \boldsymbol{\Lambda}_{r,i}$, $\mathbf{S}_i \triangleq \boldsymbol{\Lambda}_{s,i} \mathbf{V}_{s,i}^H$, and $\mathbf{D}_i \triangleq \mathbf{A}_i^H \boldsymbol{\Lambda}_{r,i} \mathbf{U}_{r,i}^H$, we can rewrite (3.36) as

$$\begin{aligned} \frac{\partial f(\mathbf{A}_i)}{\partial \mathbf{A}_i} &= \frac{\partial}{\partial \mathbf{A}_i} \text{tr}(\mathbf{M}_i (\mathbf{Z}_i + \mathbf{U}_{r,i} \boldsymbol{\Lambda}_{r,i} \mathbf{A}_i \boldsymbol{\Lambda}_{s,i} \mathbf{V}_{s,i}^H) \mathbf{E}_i^H \\ &\quad + \mathbf{M}_i (\mathbf{Y}_i + \mathbf{U}_{r,i} \boldsymbol{\Lambda}_{r,i} \mathbf{A}_i \mathbf{D}_i)) - (\mathbf{E}_i^H \mathbf{G}_i^{-1} \mathbf{U}_{r,i} \boldsymbol{\Lambda}_{r,i})^T (\boldsymbol{\Lambda}_{s,i} \mathbf{V}_{s,i}^H)^T \\ &= \frac{\partial}{\partial \mathbf{A}_i} \text{tr}(\mathbf{M}_i \mathbf{R}_i \mathbf{A}_i \mathbf{S}_i \mathbf{E}_i^H + \mathbf{M}_i \mathbf{R}_i \mathbf{A}_i \mathbf{D}_i) - (\mathbf{E}_i^H \mathbf{G}_i^{-1} \mathbf{R}_i)^T \mathbf{S}_i^T. \end{aligned} \quad (3.37)$$

Finally, the gradient of $f(\mathbf{A}_i)$ is given by

$$\begin{aligned} \nabla f(\mathbf{A}_i) &= 2 \left(\frac{\partial f(\mathbf{A}_i)}{\partial \mathbf{A}_i} \right)^* \\ &= 2((\mathbf{M}_i \mathbf{R}_i)^T (\mathbf{S}_i \mathbf{E}_i^H)^T + (\mathbf{M}_i \mathbf{R}_i)^T \mathbf{D}_i^T - (\mathbf{E}_i^H \mathbf{G}_i^{-1} \mathbf{R}_i)^T \mathbf{S}_i^T)^* \\ &= 2(\mathbf{R}_i^H \mathbf{M}_i^H (\mathbf{E}_i \mathbf{S}_i^H + \mathbf{D}_i^H) - \mathbf{R}_i^H \mathbf{G}_i^{-H} \mathbf{E}_i \mathbf{S}_i^H). \end{aligned} \quad (3.38)$$

Chapter 4

Simplified Source and Relay Matrices Design

To reduce the complexity of the algorithm in Chapters 3, we develop a simplified source and relay matrices design algorithm. We first relax the power constraint at each relay node to the power constraint at the output of the second-hop channel. We propose a jointly optimal source and relay beamforming algorithm which minimizes the MSE of signal waveform estimation at the destination node for the relaxed problem. Then we scale the relay matrices to satisfy the individual power constraint at each relay node. In Section 4.1, we show that both the optimal source precoding matrix and the optimal relay amplifying matrices have a beamforming structure. By using the optimal structure, a joint source and relay power loading algorithm is then developed to minimize the MSE of the signal waveform estimation. The simulation results in Section 4.2 demonstrate that the proposed joint source and relay beamforming algorithm has an improved performance-complexity tradeoff. The chapter is briefly summarized in Section 4.3.

4.1 MMSE Relay Design Algorithm

The communication process between the source and destination nodes for a parallel MIMO relay communication system with multiple data streams has been introduced in Chapter 3 in (3.1)-(3.5). Fig. 4.1 illustrates an equivalent two-hop MIMO relay system

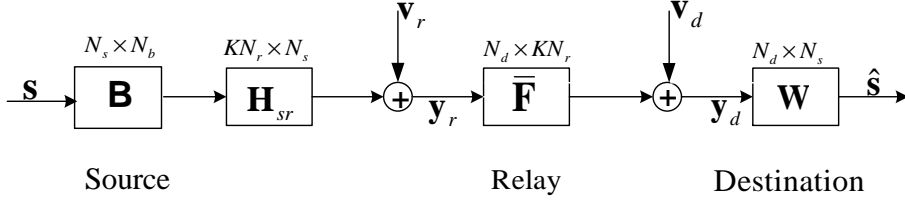


Figure 4.1: Block diagram of the equivalent MIMO relay system with multiple data streams.

with multiple data streams by introducing

$$\bar{\mathbf{F}} \triangleq \mathbf{H}_{rd}\mathbf{F}. \quad (4.1)$$

The received signal vector at the destination node can be equivalently written as

$$\mathbf{y}_d = \bar{\mathbf{F}}\mathbf{H}_{sr}\mathbf{B}\mathbf{s} + \bar{\mathbf{F}}\mathbf{v}_r + \mathbf{v}_d = \bar{\mathbf{H}}\mathbf{s} + \bar{\mathbf{v}}$$

where we define $\bar{\mathbf{H}} \triangleq \bar{\mathbf{F}}\mathbf{H}_{sr}\mathbf{B}$ as the effective MIMO channel matrix of the source-relay-destination link, and $\bar{\mathbf{v}}$ as the equivalent noise with $\bar{\mathbf{v}} \triangleq \bar{\mathbf{F}}\mathbf{v}_r + \mathbf{v}_d$. The transmission power consumed by each relay node (3.3) can be expressed in (3.6). Based on (3.6) and (3.7), the joint source and relay optimization problem with a linear MMSE receiver used at the destination node can be formulated as

$$\min_{\{\mathbf{F}_i\}, \mathbf{B}} \quad \text{tr}\left([\mathbf{I}_{N_b} + \bar{\mathbf{H}}^H\mathbf{C}_{\bar{\mathbf{v}}}^{-1}\bar{\mathbf{H}}]^{-1}\right) \quad (4.2)$$

$$\text{s.t.} \quad \text{tr}(\mathbf{B}\mathbf{B}^H) \leq P_s \quad (4.3)$$

$$\text{tr}(\mathbf{F}_i[\mathbf{H}_{sr,i}\mathbf{B}\mathbf{B}^H\mathbf{H}_{sr,i}^H + \mathbf{I}_{N_r}]\mathbf{F}_i^H) \leq P_{r,i}, \quad i = 1, \dots, K \quad (4.4)$$

where (4.3) is the transmit power constraint at the source node, while (4.4) is the power constraint at each relay node. Here $P_s > 0$ and $P_{r,i} > 0$, $i = 1, \dots, K$, are the corresponding power budget. Obviously, to avoid any loss of transmission power in the relay system when a linear receiver is used, there should be $N_b \leq \min(N_s, KN_r, N_d)$.

Due to the power constraint at each relay node (4.4), the source and relay matrices optimization problem (4.2)-(4.4) is much more challenging to solve when $K \geq 2$ compared with the case of $K = 1$. To overcome this difficulty, we relax the power constraints in (4.4) by considering the power of the signal at the output of \mathbf{H}_{rd} , which can be expressed as [73]

$$\mathbb{E}[\text{tr}((\mathbf{H}_{rd}\mathbf{x}_r)(\mathbf{H}_{rd}\mathbf{x}_r)^H)] = \text{tr}(\bar{\mathbf{F}}[\mathbf{H}_{sr}\mathbf{B}\mathbf{B}^H\mathbf{H}_{sr}^H + \mathbf{I}_{KN_r}]\bar{\mathbf{F}}^H) \leq P_r\text{tr}(\mathbf{H}_{rd}\mathbf{H}_{rd}^H). \quad (4.5)$$

Here $P_r \triangleq \sum_{i=1}^K P_{r,i}$ is the total transmission power budget available to all K relay nodes. By using (4.5), the relaxed joint source and relay optimization problem can be written as

$$\min_{\bar{\mathbf{F}}, \mathbf{B}} \quad \text{tr} \left([\mathbf{I}_{N_b} + \bar{\mathbf{H}}^H \mathbf{C}_v^{-1} \bar{\mathbf{H}}]^{-1} \right) \quad (4.6)$$

$$\text{s.t.} \quad \text{tr}(\mathbf{B}\mathbf{B}^H) \leq P_s \quad (4.7)$$

$$\text{tr}(\bar{\mathbf{F}}[\mathbf{H}_{sr}\mathbf{B}\mathbf{B}^H\mathbf{H}_{sr}^H + \mathbf{I}_{KN_r}]\bar{\mathbf{F}}^H) \leq P_x \quad (4.8)$$

where $P_x \triangleq P_r \text{tr}(\mathbf{H}_{rd}\mathbf{H}_{rd}^H)$, and (4.8) is the power constraint at the output of \mathbf{H}_{rd} .

Let $\mathbf{H}_{sr} = \mathbf{U}_s \mathbf{\Lambda}_s \mathbf{V}_s^H$ denote the singular value decomposition (SVD) of \mathbf{H}_{sr} , where the dimensions of \mathbf{U}_s , $\mathbf{\Lambda}_s$, \mathbf{V}_s are $KN_r \times KN_r$, $KN_r \times N_s$, $N_s \times N_s$, respectively. We assume that the main diagonal elements of $\mathbf{\Lambda}_s$ are arranged in a decreasing order. By using Theorem 1 in [60], the optimal structure of $\bar{\mathbf{F}}$ and \mathbf{B} as the solution to the problem (4.6)-(4.8) is given by

$$\bar{\mathbf{F}} = \mathbf{Q}\mathbf{\Lambda}_f\mathbf{U}_{s,1}^H, \quad \mathbf{B} = \mathbf{V}_{s,1}\mathbf{\Lambda}_b \quad (4.9)$$

where \mathbf{Q} is any $N_d \times N_b$ semi-unitary matrix with $\mathbf{Q}^H\mathbf{Q} = \mathbf{I}_{N_b}$, $\mathbf{U}_{s,1}$ and $\mathbf{V}_{s,1}$ contain the leftmost N_b columns of \mathbf{U}_s and \mathbf{V}_s , respectively, $\mathbf{\Lambda}_f$ and $\mathbf{\Lambda}_b$ are $N_b \times N_b$ diagonal matrices. From (4.9), we see that the optimal $\bar{\mathbf{F}}$ and \mathbf{B} have a beamforming structure. In fact, they jointly diagonalize the source-relay-destination channel $\bar{\mathbf{H}}$. By using (4.9), the joint source-relay optimization problem (4.6)-(4.8) becomes

$$\min_{\mathbf{\Lambda}_f, \mathbf{\Lambda}_b} \quad \text{tr} \left(\left[\mathbf{I}_{N_b} + (\mathbf{\Lambda}_f \mathbf{\Lambda}_s \mathbf{\Lambda}_b)^2 [\mathbf{\Lambda}_f^2 + \mathbf{I}_{N_b}]^{-1} \right]^{-1} \right) \quad (4.10)$$

$$\text{s.t.} \quad \text{tr}(\mathbf{\Lambda}_b^2) \leq P_s \quad (4.11)$$

$$\text{tr} \left(\mathbf{\Lambda}_f^2 [(\mathbf{\Lambda}_s \mathbf{\Lambda}_b)^2 + \mathbf{I}_{N_b}] \right) \leq P_x. \quad (4.12)$$

Denoting $\lambda_{f,i}$, $\lambda_{s,i}$, $\lambda_{b,i}$, $i = 1, \dots, N_b$, as the main diagonal elements of $\mathbf{\Lambda}_f$, $\mathbf{\Lambda}_s$, $\mathbf{\Lambda}_b$, respectively, the optimization problem (4.10)-(4.12) can be equivalently written as

$$\min_{\{\lambda_{f,i}\}, \{\lambda_{b,i}\}} \quad \sum_{i=1}^{N_b} \left(1 + \frac{(\lambda_{f,i} \lambda_{s,i} \lambda_{b,i})^2}{\lambda_{f,i}^2 + 1} \right)^{-1} \quad (4.13)$$

$$\text{s.t.} \quad \sum_{i=1}^{N_b} \lambda_{b,i}^2 \leq P_s \quad (4.14)$$

$$\sum_{i=1}^{N_b} \lambda_{f,i}^2 [(\lambda_{s,i} \lambda_{b,i})^2 + 1] \leq P_x \quad (4.15)$$

$$\lambda_{b,i} \geq 0, \quad \lambda_{f,i} \geq 0, \quad i = 1, \dots, N_b. \quad (4.16)$$

The problem (4.13)-(4.16) is nonconvex and a closed-form solution is intractable to obtain. In the following, we develop an iterative method to obtain a numerical solution of the optimal $\{\lambda_{f,i}\}$ and $\{\lambda_{b,i}\}$. Let us define

$$\begin{aligned} a_i &\triangleq \lambda_{s,i}^2, & x_i &\triangleq \lambda_{b,i}^2, \\ y_i &\triangleq \lambda_{f,i}^2 [(\lambda_{s,i} \lambda_{b,i})^2 + 1], & i &= 1, \dots, N_b. \end{aligned} \quad (4.17)$$

Then the optimization problem (4.13)-(4.16) can be equivalently rewritten as

$$\min_{\{x_i\}, \{y_i\}} \sum_{i=1}^{N_b} \left(1 + \frac{\frac{a_i x_i y_i}{a_i x_i + 1}}{1 + \frac{y_i}{a_i x_i + 1}} \right)^{-1} \quad (4.18)$$

$$\text{s.t.} \quad \sum_{i=1}^{N_b} x_i \leq P_s \quad (4.19)$$

$$\sum_{i=1}^{N_b} y_i \leq P_x \quad (4.20)$$

$$x_i \geq 0, \quad y_i \geq 0, \quad i = 1, \dots, N_b. \quad (4.21)$$

For a fixed $\{y_i\}$ satisfying (4.20) and (4.21), the problem of optimizing $\{x_i\}$ can be written as

$$\min_{\{x_i\}} \sum_{i=1}^{N_b} \frac{a_i x_i + y_i + 1}{a_i x_i y_i + a_i x_i + y_i + 1} \quad (4.22)$$

$$\text{s.t.} \quad \sum_{i=1}^{N_b} x_i \leq P_s \quad (4.23)$$

$$x_i \geq 0, \quad i = 1, \dots, N_b. \quad (4.24)$$

The Lagrangian function associated with the problem (4.22)-(4.24) can be written as

$$\mathcal{L} = \sum_{i=1}^{N_b} \frac{a_i x_i + y_i + 1}{a_i x_i y_i + a_i x_i + y_i + 1} + \mu_1 \left(\sum_{i=1}^{N_b} x_i - P_s \right) \quad (4.25)$$

where $\mu_1 \geq 0$ is the Lagrangian multiplier. Taking the derivative of (4.25) with respect to x_i equal to zero, we obtain

$$x_i = \frac{1}{a_i} \left[\sqrt{\frac{a_i y_i}{\mu_1 (y_i + 1)}} - 1 \right]^\dagger, \quad i = 1, \dots, N_b$$

where μ_1 is the solution to the following nonlinear equation

$$\sum_{i=1}^{N_b} \frac{1}{a_i} \left[\sqrt{\frac{a_i y_i}{\mu_1 (y_i + 1)}} - 1 \right]^\dagger = P_s.$$

In a similar fashion, for a fixed $\{x_i\}$ satisfying (4.19) and (4.21), we can update $\{y_i\}$ as

$$y_i = \left[\sqrt{\frac{a_i x_i}{\mu_2 (a_i x_i + 1)}} - 1 \right]^\dagger, \quad i = 1, \dots, N_b$$

where $\mu_2 \geq 0$ is the solution to the following nonlinear equation

$$\sum_{i=1}^{N_b} \left[\sqrt{\frac{a_i x_i}{\mu_2 (a_i x_i + 1)}} - 1 \right]^\dagger = P_x.$$

Note that the conditional updates of $\{x_i\}$ and $\{y_i\}$ may either decrease or maintain but cannot increase the objective function in (4.18). Monotonic convergence of $\{x_i\}$ and $\{y_i\}$ follows directly from this observation. After the convergence of the alternating algorithm, $\lambda_{f,i}$ and $\lambda_{b,i}$ can be obtained from (4.17) as

$$\lambda_{f,i} = \sqrt{\frac{y_i}{\lambda_{s,i}^2 x_i + 1}}, \quad \lambda_{b,i} = \sqrt{x_i}, \quad i = 1, \dots, N_b.$$

By using (4.1) and the optimal structure of $\bar{\mathbf{F}}$ and \mathbf{B} in (4.9), we have $\mathbf{H}_{rd,i} \mathbf{F}_i = \mathbf{Q} \mathbf{\Lambda}_f \mathbf{\Phi}_i$, where matrix $\mathbf{\Phi}_i$ contains the $(i-1)N_r + 1$ to iN_r columns of $\mathbf{U}_{s,1}^H$. Then we obtain

$$\mathbf{F}_i = \mathbf{H}_{rd,i}^+ \mathbf{Q} \mathbf{\Lambda}_f \mathbf{\Phi}_i, \quad i = 1, \dots, K. \quad (4.26)$$

Finally, we scale \mathbf{F}_i in (4.26) to satisfy the power constraint (4.4) at each relay node as

$$\tilde{\mathbf{F}}_i = \alpha_i \mathbf{F}_i, \quad i = 1, \dots, K \quad (4.27)$$

where the scaling factor α_i is given by

$$\alpha_i = \sqrt{\frac{P_{r,i}}{\text{tr}(\mathbf{F}_i [\mathbf{H}_{sr,i} \mathbf{B} \mathbf{B}^H \mathbf{H}_{sr,i}^H + \mathbf{I}_{N_r}] \mathbf{F}_i^H)}}, \quad i = 1, \dots, K. \quad (4.28)$$

4.2 Numerical Examples

In this section, we study the performance of the proposed simplified joint source and relay beamforming algorithm for parallel MIMO relay communication systems with multiple parallel relay nodes. All simulations are conducted in a flat Rayleigh fading environment using the BPSK constellation, and the noises are i.i.d. Gaussian with zero mean and unit variance. The channel matrices have zero-mean entries with variances σ_s^2/N_s and $\sigma_r^2/(KN_r)$ for \mathbf{H}_{sr} and \mathbf{H}_{rd} , respectively. We vary the SNR in the source-to-relay link (SNR_s) while fixing the SNR in the relay-to-destination link (SNR_r) to 20dB.

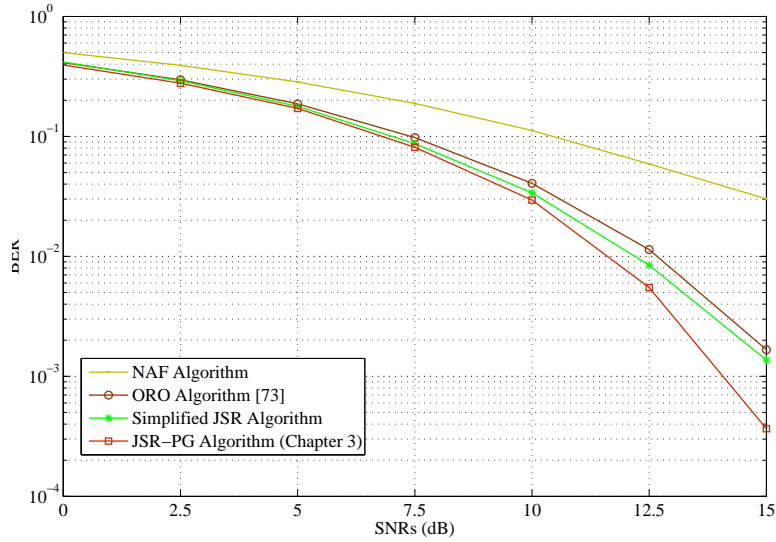


Figure 4.2: Example 4.1 BER versus SNR_s with $K = 3$.

We transmit 1000 randomly generated bits in each channel realization, and the BER results are averaged through 200 channel realizations. Here we set $N_b = N_s = N_r = N_d = 3$.

In the first example, we simulate a relay system with $K = 3$ and compare the BER performance of the following algorithms: (i) the proposed simplified joint source and relay scheme (Simplified JSR); (ii) joint source and relay optimization algorithm using the projected gradient (JSR-PG, Chapter 3); (iii) the NAF algorithm where both the source and relay matrices are scaled identity matrices satisfying power constraints (4.7) and (4.8); (iv) the optimal relay only (ORO) algorithm developed in [73] where the relay matrices are optimized based on the MMSE criterion, while the source precoding matrix is a scaled identity matrix. Fig. 4.2 shows the BER performance of four systems versus SNR_s . It can be seen from Fig. 4.2 that the NAF algorithm has the worst performance, since it does not exploit the channel knowledge available. The proposed algorithm has a higher BER than the algorithm in Chapter 3. However, the former algorithm has a much lower computational complexity than the latter one.

In the second example, we study the effect of the number of relays to the system BER performance using the proposed algorithm. Fig. 4.3 displays the system BER versus SNR_s with $K = 2, 3$, and 5. It can be seen that at $\text{BER} = 10^{-2}$, for proposed simplified algorithm, we can achieve approximately 4.5dB gain by increasing from $K = 2$ to $K = 5$.

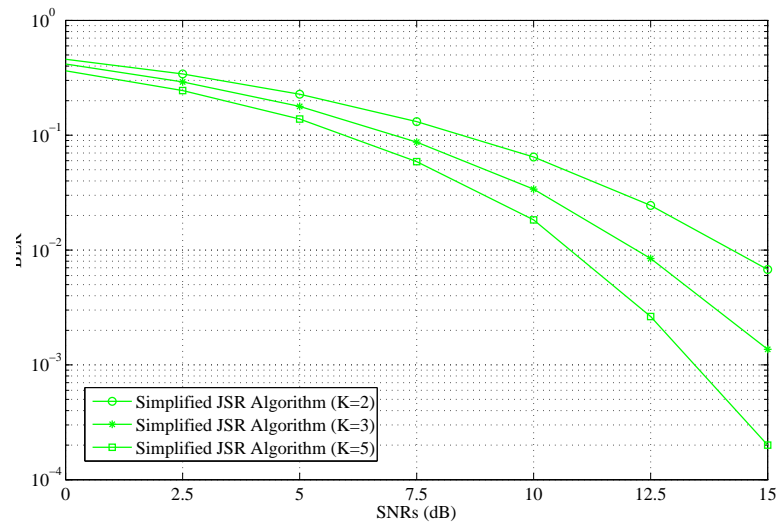


Figure 4.3: Example 4.2 BER versus SNR_s with varying K .

4.3 Chapter Summary

In this chapter, we have proposed a simplified source and relay matrices design algorithm for parallel MIMO relay communication systems with multiple parallel data streams. The proposed algorithm has an improved performance-complexity tradeoff.

Chapter 5

Parallel MIMO Relay Design Based on Nonlinear Receiver

In this chapter, we study the optimal structure of the source precoding matrix and the relay amplifying matrices for parallel MIMO relay communication systems with multiple data streams when a nonlinear DFE receiver is used at the destination node, and the MMSE criterion is used to detect the transmitted signal at each stream.

The rest of the chapter is organized as follows. Existing works are briefly summarized in Section 5.1 which is followed by performance comparison of the linear and the nonlinear receivers in Section 5.2. We show that the optimal source precoding matrix and the optimal relay amplifying matrices have a beamforming structure in Section 5.3. Using such optimal source and relay matrices and the MMSE-DFE receiver, a joint source and relay power loading algorithm is developed to minimize the MSE of the signal waveform estimation. In Section 5.4, numerical simulations are performed to demonstrate the performance of the proposed algorithm. The chapter is summarized in Section 5.5.

5.1 Overview of Known Techniques

It is well known that relay techniques are very efficient in enhancing the coverage and the energy efficiency of wireless communication systems [3, 4]. When nodes in the relay system are installed with multiple antennas, we call such system MIMO relay communication system. MIMO relay communication systems have attracted much research

interest and provided significant improvement in terms of both spectral efficiency and link reliability [12, 37, 38, 47, 54, 57–60, 73, 74, 89]. In [12, 38, 54, 57–60], the authors have studied MIMO relay systems with a single relay node at each hop. MIMO relay systems with multiple parallel relay nodes have been investigated in [73] and Chapters 2-4. In [73], the optimal relay amplifying matrices are developed to minimize the MSE of the signal waveform estimation. In Chapters 2-4, we investigated the jointly optimal structure of the source precoding matrix and the relay amplifying matrices when a linear MMSE receiver is used at the destination node.

In this chapter, we study MIMO parallel relay systems with a nonlinear DFE at the destination node. In particular, the MMSE criterion is used to estimate the transmitted signal at each stream. We call such receiver an MMSE-DFE receiver. We show that the optimal relay amplifying matrices have a beamforming structure. This result generalizes the optimal source and relay matrices design from a linear MMSE receiver case Chapter 4 to nonlinear MMSE-DFE receiver scenarios. Simulation results show that the proposed source and relay matrices together with the MMSE-DFE receiver yield a significant BER performance improvement compared with the linear MMSE based relay algorithm developed in Chapter 4.

5.2 Performance Comparison of Linear and Nonlinear Receivers

The basic MIMO relay system with SIC technique is illustrated in Fig. 1.1. In this section, we compare the performance of the MIMO relay systems with linear and nonlinear receivers through numerical simulations. In the simulations, the transmission signaling is in spatial multiplexing mode (i.e., the source transmits independent data streams from different antennas) with total transmit power uniformly distributed among the transmit antennas. We define the relay amplifying matrices as scaled identity matrices satisfying the power constraints at the relay nodes. Also, all simulations are conducted in a flat-fading Rayleigh environment using the BPSK constellation, and the noise variances are assumed to be the same for all antennas. We transmitted 10^3 randomly generated bits in each channel realization and the BER results are averaged through 200 channel realizations. We plot BER curves versus SNR.

In the first example, we simulate the system BER performance of ZF and MMSE receiver with and without SIC in MIMO relay channel with varying SNR in the source-

to-relay link (SNR_s) keeping the relay-to-destination link (SNR_r) at 20dB. Fig. 5.1 show the BER performance with $N_s = N_r = N_d = 2$, $K = 1$. It can be seen that at $BER = 10^{-3}$, we achieve 5 dB gain from MMSE to MMSE-SIC as well as from ZF to ZF-SIC.

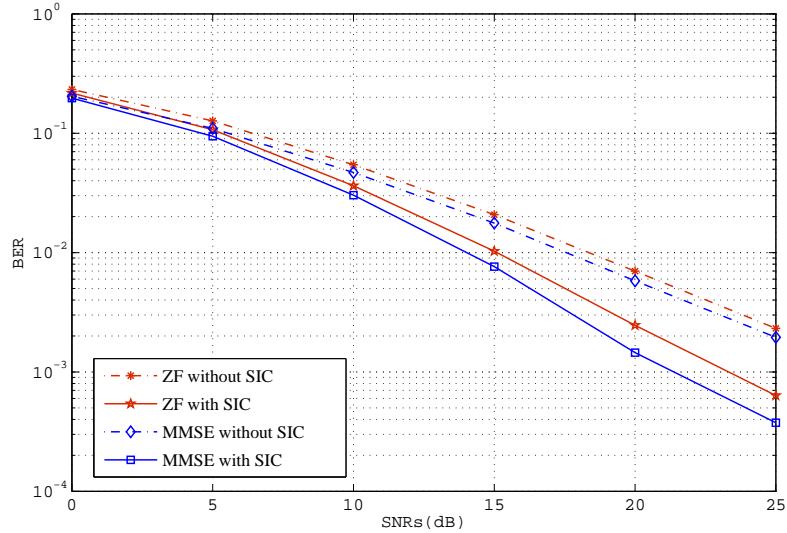


Figure 5.1: BER versus SNR_s . $N_s = N_r = N_d = 2$, $K = 1$ and $SNR_r = 20$ dB for MIMO relay channel.

In the second example, we simulate the system BER performance of ZF and MMSE receiver with and without SIC in MIMO relay channel with varying SNR in the relay-to-destination link (SNR_r) keeping the source-to-relay link (SNR_s) at 20dB. Fig. 5.2 show the BER performance with $N_s = N_r = N_d = 2$, $K = 1$. Our results demonstrate that ZF-SIC and MMSE-SIC receiver algorithms have lower BER compared to the ZF and MMSE receiver algorithms.

5.3 Optimal Source and Relay Design with DFE

Fig. 1.1 illustrates a two-hop parallel MIMO relay communication system consisting of one source node, K parallel relay nodes, and one destination node. We assume that the source and destination nodes have N_s and N_d antennas, respectively, and each relay node has N_r antennas.

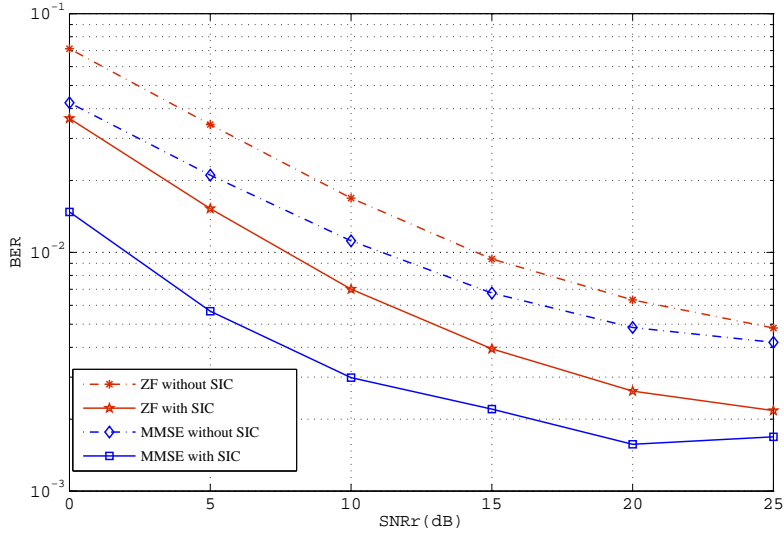


Figure 5.2: BER versus SNR_r . $N_s = N_r = N_d = 2$, $K = 1$ and $SNR_s = 20$ dB for MIMO relay channel.

The communication process between the source and destination nodes for MIMO relay system has been introduced in Chapter 3 (3.1)-(3.6), and Chapter 4 (4.1).

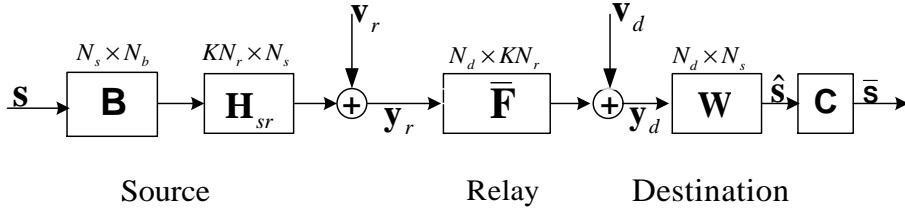


Figure 5.3: Block diagram of the equivalent MIMO relay system with SIC technique.

At the destination node, a nonlinear DFE receiver is used to detect the source symbols successively with the N_b th symbol detected first and the first symbol detected last. The equivalent MIMO relay system model is shown in Fig. 5.3. Assuming that there is no error propagation in the DFE receiver, the k th source symbol is estimated

as

$$\bar{s}_k = \bar{\mathbf{w}}_k^H \mathbf{y}_d - \sum_{l=k+1}^{N_b} c_{k,l} s_l, \quad k = 1, \dots, N_b \quad (5.1)$$

where $\bar{\mathbf{w}}_k$ is the feed-forward vector for the k th symbol, and $c_{k,l}$, $l = k+1, \dots, N_b$, are the feedback coefficients for the k th symbol. By introducing $\bar{\mathbf{W}} = [\bar{\mathbf{w}}_1, \bar{\mathbf{w}}_2, \dots, \bar{\mathbf{w}}_{N_b}]$, $\bar{\mathbf{s}} = [\bar{s}_1, \bar{s}_2, \dots, \bar{s}_{N_b}]^T$, and an $N_b \times N_b$ strictly upper-triangular matrix \mathbf{C} with nonzero elements $c_{k,l}$, we can represent (5.1) in matrix form as

$$\bar{\mathbf{s}} = \bar{\mathbf{W}}^H \mathbf{y}_d - \mathbf{C} \bar{\mathbf{s}} = (\bar{\mathbf{W}}^H \bar{\mathbf{H}} - \mathbf{C}) \bar{\mathbf{s}} + \bar{\mathbf{W}}^H \bar{\mathbf{v}} \quad (5.2)$$

where $\bar{\mathbf{W}}$ and \mathbf{C} are the feed-forward matrix and the feedback matrix of the DFE receiver, respectively. To minimize error of the signal estimation in (5.2), we get

$$\mathbf{C} = \mathcal{U}[\bar{\mathbf{W}}^H \bar{\mathbf{H}}] \quad (5.3)$$

where $\mathcal{U}[\bar{\mathbf{W}}^H \bar{\mathbf{H}}]$ denotes the strictly upper-triangular part of $\bar{\mathbf{W}}^H \bar{\mathbf{H}}$. Substituting (5.3) back into (5.1), we obtain

$$\bar{s}_k = \bar{\mathbf{w}}_k^H ([\bar{\mathbf{H}}]_{1:k} [\mathbf{s}]_{1:k} + \bar{\mathbf{v}}), \quad k = 1, \dots, N_b \quad (5.4)$$

where $[\mathbf{a}]_{1:k}$ denotes a vector containing the first k elements of vector \mathbf{a} , and $[\mathbf{A}]_{1:k}$ stands for a matrix containing the first k columns of \mathbf{A} .

When the MMSE criterion is used to estimate each symbol, from (5.4) the feed-forward matrix $\bar{\mathbf{W}}$ is given as

$$\bar{\mathbf{w}}_k = ([\bar{\mathbf{H}}]_{1:k} [\bar{\mathbf{H}}]_{1:k}^H + \mathbf{C}_{\bar{v}})^{-1} \bar{\mathbf{h}}_k, \quad k = 1, \dots, N_b$$

where $\bar{\mathbf{h}}_k$ is the k th column of $\bar{\mathbf{H}}$. Let us introduce the following QR decomposition

$$\mathbf{G} \triangleq \begin{bmatrix} \mathbf{C}_{\bar{v}}^{-1/2} \bar{\mathbf{H}} \\ \mathbf{I}_{N_b} \end{bmatrix} = \mathbf{Q} \mathbf{R} = \begin{bmatrix} \bar{\mathbf{Q}} \\ \underline{\mathbf{Q}} \end{bmatrix} \mathbf{R} \quad (5.5)$$

where \mathbf{R} is an $N_b \times N_b$ upper-triangular matrix with all positive diagonal elements, \mathbf{Q} is an $(N_b + N_d) \times N_b$ semi-unitary matrix with $\mathbf{Q}^H \mathbf{Q} = \mathbf{I}_{N_b}$, $\bar{\mathbf{Q}}$ is a matrix containing the first N_d rows of \mathbf{Q} , and $\underline{\mathbf{Q}}$ contains the last N_b rows of \mathbf{Q} .

Using the QR decomposition (5.5), it has been shown in [89] that the feed-forward weight matrix $\bar{\mathbf{W}}$, the feedback matrix \mathbf{C} and the MSE matrix $\mathbf{E} = \mathbb{E}[(\bar{\mathbf{s}} - \mathbf{s})(\bar{\mathbf{s}} - \mathbf{s})^H]$ can be written as

$$\bar{\mathbf{W}} = \mathbf{C}_{\bar{v}}^{-1/2} \bar{\mathbf{Q}} \mathbf{D}_R^{-1}, \quad \mathbf{C} = \mathbf{D}_R^{-1} \mathbf{R} - \mathbf{I}_{N_b}, \quad \mathbf{E} = \mathbf{D}_R^{-2} \quad (5.6)$$

where \mathbf{D}_R is a matrix taking the diagonal elements of \mathbf{R} as the main diagonal and zero elsewhere. Using (5.5) and (5.6), the joint source and relay optimization problem which minimizes the MSE of the signal waveform estimation can be formulated as

$$\min_{\bar{\mathbf{F}}, \mathbf{B}} \quad \text{tr}(\mathbf{D}_R^{-2}) \quad (5.7)$$

$$\text{s.t.} \quad \begin{bmatrix} \mathbf{C}_{\bar{\mathbf{v}}}^{-1/2} \bar{\mathbf{H}} \\ \mathbf{I}_{N_b} \end{bmatrix} = \mathbf{Q}\mathbf{R} \quad (5.8)$$

$$\text{tr}(\mathbf{B}\mathbf{B}^H) \leq P_s \quad (5.9)$$

$$\text{tr}(\bar{\mathbf{F}}[\mathbf{H}_{sr}\mathbf{B}\mathbf{B}^H\mathbf{H}_{sr}^H + \mathbf{I}_{N_r}]\bar{\mathbf{F}}^H) \leq P_x \quad (5.10)$$

where (5.9) is the transmit power constraint at the source node, while (5.10) is the power constraint at the output of \mathbf{H}_{rd} (Chapter 4). Here $P_x > 0$ and $P_s > 0$ are the corresponding power budgets.

Let $\mathbf{H}_{sr} = \mathbf{U}_s \mathbf{\Lambda}_s \mathbf{V}_s^H$ denote the singular value decomposition (SVD) of \mathbf{H}_{sr} , where the dimensions of \mathbf{U}_s , $\mathbf{\Lambda}_s$, \mathbf{V}_s are $KN_r \times KN_r$, $KN_r \times N_s$, $N_s \times N_s$, respectively. We assume that the main diagonal elements of $\mathbf{\Lambda}_s$ are arranged in a decreasing order. We also introduce $M = \min(R_h, N_b)$, where $R_h \triangleq \min(\text{rank}(\mathbf{H}_{sr}), \text{rank}(\mathbf{H}_{rd}))$. Using the nonlinear MMSE-DFE receiver at the destination node of a parallel MIMO relay network, the optimal source precoding matrix and the relay amplifying matrices as the solution to the problem (5.7)-(5.10) are given by

$$\bar{\mathbf{F}} = \mathbf{V}\mathbf{\Lambda}_f\mathbf{U}_{s,1}^H, \quad \mathbf{B} = \mathbf{V}_{s,1}\mathbf{\Lambda}_b\mathbf{V}_r^H \quad (5.11)$$

where $\mathbf{\Lambda}_f$ and $\mathbf{\Lambda}_b$ are $M \times M$ diagonal matrices, \mathbf{V} is any $N_d \times M$ semi-unitary matrix with $\mathbf{V}^H\mathbf{V} = \mathbf{I}_M$, $\mathbf{U}_{s,1}$ and $\mathbf{V}_{s,1}$ contain the leftmost M vectors of \mathbf{U}_s and \mathbf{V}_s , respectively, and \mathbf{V}_r is an $N_b \times M$ semi-unitary matrix ($\mathbf{V}_r^H\mathbf{V}_r = \mathbf{I}_M$) such that the QR decomposition in (5.8) holds. The proof of (5.11) is similar to the proof of Theorem 2 in [89].

From (5.11), we find that both $\bar{\mathbf{F}}$ and \mathbf{B} have a beamforming structure. In particular, they jointly diagonalize the source-relay-destination channel matrix $\bar{\mathbf{H}}$ up to rotational matrices \mathbf{V} and \mathbf{V}_r . It can be shown similar to [89] that the constraint (5.8) can be equivalently written as

$$\mathbf{d}[\mathbf{D}_R] \prec \boldsymbol{\sigma}_G \quad (5.12)$$

where \prec stands for multiplicative majorization [109], $\boldsymbol{\sigma}_G$ is a column vector containing singular values of \mathbf{G} , and $\mathbf{d}[\mathbf{D}_R]$ is a column vector containing all diagonal elements of

\mathbf{D}_R . Let us denote $\lambda_{f,i}, \lambda_{s,i}, \lambda_{b,i}$, $i = 1, \dots, M$, as the main diagonal elements of $\mathbf{\Lambda}_f$, $\mathbf{\Lambda}_s$, $\mathbf{\Lambda}_b$, respectively. Using (5.11) and (5.12), the optimization problem (5.7)-(5.10) can be equivalently rewritten as

$$\min_{\{\lambda_{f,i}\}, \{\lambda_{b,i}\}} \text{tr}(\mathbf{D}_R^{-2}) \quad (5.13)$$

$$\text{s.t. } \mathbf{d}[\mathbf{D}_R^2] \prec_w \left[\left\{ 1 + \frac{(\lambda_{f,i} \lambda_{s,i} \lambda_{b,i})^2}{\lambda_{f,i}^2 + 1} \right\}^T, \mathbf{1}_{N_b - M} \right]^T \quad (5.14)$$

$$\sum_{i=1}^M \lambda_{b,i}^2 \leq P_s \quad (5.15)$$

$$\sum_{i=1}^M \lambda_{f,i}^2 [(\lambda_{s,i} \lambda_{b,i})^2 + 1] \leq P_x \quad (5.16)$$

$$\lambda_{b,i} \geq 0, \quad \lambda_{f,i} \geq 0, \quad i = 1, \dots, M \quad (5.17)$$

where \prec_w stands for weakly multiplicative submajorization [109], $\{a\}$ stands for an $M \times 1$ vector $[a_1, a_2, \dots, a_M]^T$, $\mathbf{1}_{N_b - M}$ denotes a $1 \times (N_b - M)$ vector with all 1 elements.

The problem (5.13)-(5.17) is highly nonconvex and a closed-form solution is intractable to obtain. In the following, we develop an iterative method to obtain a numerical solution of the optimal $\{\lambda_{f,i}\}$ and $\{\lambda_{b,i}\}$. Let us define

$$\begin{aligned} a_i &\triangleq \lambda_{s,i}^2, & x_i &\triangleq \lambda_{b,i}^2, \\ y_i &\triangleq \lambda_{f,i}^2 [(\lambda_{s,i} \lambda_{b,i})^2 + 1], & i &= 1, \dots, M. \end{aligned} \quad (5.18)$$

Then using the definition of the operator \prec_w in [109], the optimization problem (5.13)-(5.17) can be equivalently written as

$$\min_{\{x_i\}, \{y_i\}} - \sum_{i=1}^M \log \left(1 + \frac{\frac{a_i x_i y_i}{a_i x_i + 1}}{1 + \frac{y_i}{a_i x_i + 1}} \right) \quad (5.19)$$

$$\text{s.t. } \sum_{i=1}^M x_i \leq P_s \quad (5.20)$$

$$\sum_{i=1}^M y_i \leq P_x \quad (5.21)$$

$$x_i \geq 0, \quad y_i \geq 0, \quad i = 1, \dots, M. \quad (5.22)$$

For a $\{y_i\}$ fixed satisfying (5.21) and (5.22), the problem of optimizing $\{x_i\}$ can be

written as

$$\min_{\{x_i\}} \sum_{i=1}^M \log \left(\frac{a_i x_i + y_i + 1}{a_i x_i y_i + a_i x_i + y_i + 1} \right) \quad (5.23)$$

$$\text{s.t.} \quad \sum_{i=1}^M x_i \leq P_s \quad (5.24)$$

$$x_i \geq 0, \quad i = 1, \dots, M. \quad (5.25)$$

The Lagrangian function associated with the problem (5.23)-(5.25) can be written as

$$\mathcal{L} = \sum_{i=1}^M \log \left(\frac{a_i x_i + y_i + 1}{a_i x_i y_i + a_i x_i + y_i + 1} \right) + \mu_1 \left(\sum_{i=1}^M x_i - P_s \right) \quad (5.26)$$

where $\mu_1 \geq 0$ is the Lagrangian multiplier. Taking the derivative of (5.26) with respect to x_i equal to zero, we obtain

$$x_i = \frac{1}{2a_i} \left[\sqrt{y_i^2 + \frac{4a_i y_i}{\mu_1}} - y_i - 2 \right]^\dagger, \quad i = 1, \dots, M$$

where μ_1 is the solution to the following nonlinear equation

$$\sum_{i=1}^M \frac{1}{a_i} \left[\sqrt{y_i^2 + \frac{4a_i y_i}{\mu_1}} - y_i - 2 \right]^\dagger = 2P_s.$$

In a similar fashion, for a $\{x_i\}$ fixed satisfying (5.20) and (5.22), we can update $\{y_i\}$ as

$$y_i = \frac{1}{2} \left[\sqrt{a_i^2 x_i^2 + \frac{4a_i x_i}{\mu_2}} - a_i x_i - 2 \right]^\dagger, \quad i = 1, \dots, M$$

where $\mu_2 \geq 0$ is the solution to the following nonlinear equation

$$\sum_{i=1}^M \left[\sqrt{a_i^2 x_i^2 + \frac{4a_i x_i}{\mu_2}} - a_i x_i - 2 \right]^\dagger = 2P_x.$$

The iterative algorithm can be initialized at any random feasible \mathbf{x} or \mathbf{y} . Since the conditional updates of $\{x_i\}$ and $\{y_i\}$ may either decrease or maintain but cannot increase the objective function in (5.19). Monotonic convergence of $\{x_i\}$ and $\{y_i\}$ to a locally optimum solution follows directly from this observation. After the convergence of the alternating algorithm, $\lambda_{f,i}$ and $\lambda_{b,i}$ can be obtained from (5.18) as

$$\lambda_{f,i} = \sqrt{\frac{y_i}{a_i x_i + 1}}, \quad \lambda_{b,i} = \sqrt{x_i}, \quad i = 1, \dots, M$$

and then the optimal structure of $\bar{\mathbf{F}}$ and \mathbf{B} is given by (5.11). The rotation matrix \mathbf{V}_r in (5.11) can be computed using the numerical method developed in [110]. From (5.11), we have $\mathbf{H}_{rd,i}\mathbf{F}_i = \mathbf{V}\mathbf{\Lambda}_f\mathbf{U}_{s,i}^H$, where matrix $\mathbf{U}_{s,i}^H$ contains the $(i-1)N_r + 1$ to iN_r columns of \mathbf{U}_s^H . Then we obtain

$$\mathbf{F}_i = (\mathbf{H}_{rd,i})^+ \mathbf{V}\mathbf{\Lambda}_f\mathbf{U}_{s,i}^H, \quad i = 1, \dots, K. \quad (5.27)$$

Finally, we scale \mathbf{F}_i in (5.27) to satisfy the power constraint (4.4) at each relay node as (4.27) and (4.28).

5.4 Numerical Examples

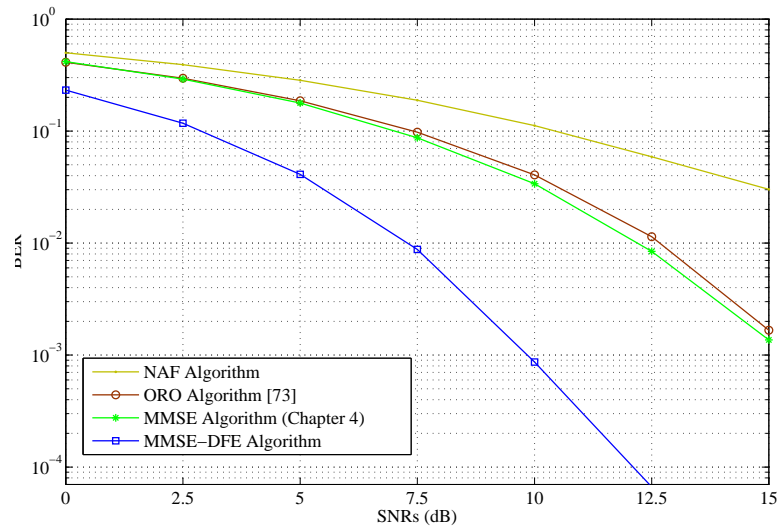


Figure 5.4: Example 5.1 BER versus SNR_s with $K = 3$.

In this section, we study the performance of the proposed optimal joint source and relay beamforming algorithm for parallel MIMO relay systems with MMSE-DFE receiver at the destination node. All simulations are conducted in a flat Rayleigh fading environment using the BPSK constellation, and the noises are i.i.d. Gaussian with zero mean and unit variance. The channel matrices have zero-mean entries with variances σ_s^2/N_s and $\sigma_r^2/(KN_r)$ for \mathbf{H}_{sr} and \mathbf{H}_{rd} , respectively. We vary the SNR in the source-to-relay link (SNR_s) while fixing the SNR in the relay-to-destination link (SNR_r) to 20dB. We transmit 1000 randomly generated bits in each channel realization, and the BER

results are averaged through 200 channel realizations. Here we set $N_b = N_s = N_r = N_d = 3$.

In the first example, we simulate $K = 3$ and compare the BER performance of the following algorithms: (i) the proposed joint source and relay scheme with MMSE-DFE receiver; (ii) the joint source and relay algorithm for parallel MIMO relay systems where a linear MMSE receiver is applied at the destination node (Chapter 4); (iii) the NAF algorithm where both the source and relay matrices are scaled identity matrices; (iv) the ORO algorithm developed in [73] where the relay matrices are optimized based on the MMSE criterion, while the source precoding matrix is a scaled identity matrix. From Fig. 5.4, it can be seen that the NAF algorithm has the worst performance. The proposed algorithm outperforms the other three approaches.

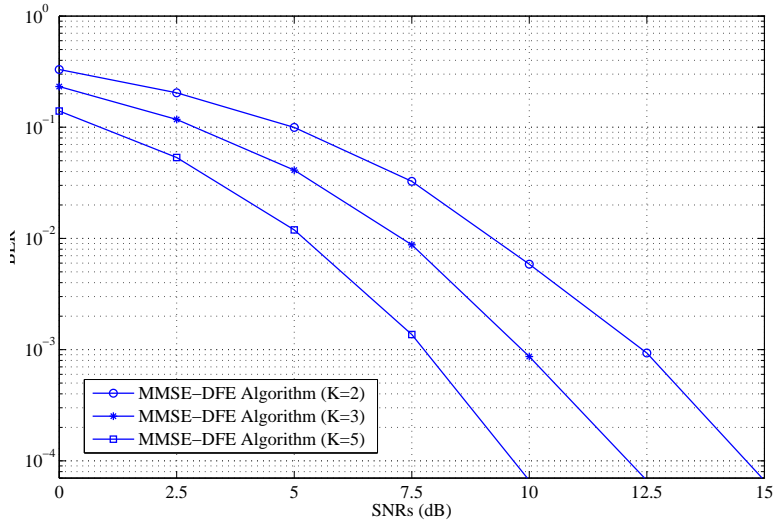


Figure 5.5: Example 5.2 BER versus SNR_s with varying K .

In the second example, we study the effect of the number of relays to the system BER performance using the proposed algorithm with MMSE-DFE receiver. Fig. 5.5 shows the BER performance with $K = 2, 3$, and 5. It can be seen that at $\text{BER} = 10^{-3}$, we achieve a 5dB gain by increasing from $K = 2$ to $K = 5$.

5.5 Chapter Summary

In this chapter, we have studied the optimal structure of the source precoding matrix and the relay amplifying matrices for parallel MIMO relay communication systems with

multiple parallel data streams when a nonlinear MMSE-DFE receiver is used at the destination node. The proposed source and relay matrices jointly diagonalize the source-relay-destination channel up to two rotation matrices and minimize the MSE of the signal waveform estimation. The proposed algorithm has an improved BER performance compared with existing techniques.

Chapter 6

Conclusions and Future Work

In wireless communications, MIMO relay communication systems have attracted much research interest and provided significant improvement in terms of both spectral efficiency and link reliability. In this thesis, we have developed several advanced algorithms for MIMO relay communication systems using parallel relays and successive interference cancellation technique.

6.1 Concluding Remarks

In Chapter 2, we studied the optimal transmit beamforming vector and the relay amplifying factors design problem for a parallel MIMO relay communication system with distributed single-antenna relay nodes when a single data stream is transmitted from the source to destination node. The proposed algorithm minimizes the MSE of the signal waveform estimation at the destination node. Simulation results demonstrate the performance of the proposed algorithm.

In Chapter 3, we have studied the general structure of the optimal source precoding matrix and relay amplifying matrices for a linear non-regenerative parallel MIMO relay communication system with multiple parallel data streams using the projected gradient approach. Simulation results demonstrate that the proposed algorithm has improved BER performance compared with the conventional techniques.

To reduce the complexity of the algorithm in the Chapter 3, we propose a simplified source and relay matrices design in Chapter 4 by first relaxing the power constraints at each relay node to the power constraint at the output of the second-hop channel. After solving the relaxed optimisation problem, the relay matrices are then scaled to

satisfy the individual power constraint at each relay node. Simulation results show a good performance-complexity tradeoff of the simplified algorithm.

Finally, in Chapter 5, we investigated the advantages of using detection algorithms in combination with SIC technique in MIMO relay communication systems and has derived the optimal structure of the source precoding matrix and the relay amplifying matrices for parallel MIMO relay communication systems with multiple parallel data streams when the nonlinear MMSE-DFE receiver is used at the destination node. Our results demonstrate that ZF-SIC and MMSE-SIC receiver algorithms outperform the ZF and MMSE receiver algorithms. The proposed optimal source precoding matrix and relay amplifying matrices together with the MMSE-DFE receiver algorithm has an improved BER performance compared with existing techniques.

6.2 Future Works

In this thesis, we have developed several advanced algorithms for MIMO relay communication systems using parallel relays and successive interference cancelation technique. However, there are still many possibilities for extending this dissertation work. We have proposed an iterative algorithm in Chapter 2 for distributed single-antenna relay nodes in a parallel MIMO relay communication system. Any possible closed-form solution to the problem can be an interesting future work since the complexity of iterative algorithms is comparatively higher than closed-form solutions.

We have extended the existing two-hop MIMO relay communication systems with single relay node schemes to two-hop MIMO relay communication systems with multiple parallel relay nodes schemes in Chapters 3-4 for linear receiver and in Chapter 5 for nonlinear receiver. However, the extension to multiple hops with parallel MIMO relay nodes still remains open as a challenging problem. Any closed form solution to the iterative algorithm proposed in Chapter 5 is also desirable.

Finally, we assumed that the channel state information (CSI) is fully known in all our algorithms. But in practice, CSI is not always perfectly known and has to be estimated. Therefore, optimal solutions robust to channel uncertainties for the problems we have solved will be of practical interest.

Bibliography

- [1] E. C. V. D. Meulen, “Three terminal communication channels,” *Adv. Appl. Prob.*, vol. 3, pp. 120–154, 1971.
- [2] T. M. Cover and A. A. El Gamal, “Capacity theorems for the relay channel,” *IEEE Trans. Inf. Theory*, vol. 25, pp. 572–584, Sep. 1979.
- [3] H. Bolukbasi, H. Yanikomeroglu, D. D. Falconer, and S. Periyalwar, “On the capacity of cellular fixed relay networks,” in *Proc. Canadian Conf. Electrical and Computer Eng.*, pp. 2217–2220, vol. 4, May 2004.
- [4] R. Pabst, B. H. Walke, D. C. Schultz, D. C. Herhold, H. Yanikomeroglu, S. Mukherjee, H. Viswanathan, M. Lott, W. Zirwas, M. Dohler, H. Aghvami, D. D. Falconer, and G. P. Fettweis, “Relay-based deployment concepts for wireless and mobile broadband radio,” *IEEE Commun. Mag.*, vol. 42, pp. 80–89, Sep. 2004.
- [5] H. Hu, H. Yanikomeroglu, D. D. Falconer, and S. Periyalwar, “Range extension without capacity penalty in cellular networks with digital fixed relays,” in *Proc. IEEE GLOBECOM*, Nov. 29-Dec. 3, 2004, vol. 5, pp. 3053–3057.
- [6] I. Kang, W. Sheen, R. Chen, and S. L. C. Hsiao, “Throughput improvement with relay-augmented cellular architecture,” *IEEE 802.16mmr-05 008*, <http://www.wirelessman.org>, Sep. 2005.
- [7] L. L. Xie and P. R. Kumar, “An achievable rate for the multiple-level relay channel,” *IEEE Trans. Inf. Theory*, vol. 51, pp. 1348–1358, Apr. 2005.
- [8] V. Havary-Nassab, S. Shahbazpanahi, A. Grami, and Z.-Q. Luo, “Distributed beamforming for relay networks based on second-order statistics of the channel

- state information,” *IEEE Trans. Signal Process.*, vol. 56, pp. 4306–4316, Sep. 2008.
- [9] M. S. Alouini and A. J. Goldsmith, “Capacity of rayleigh fading channels under different adaptive transmission and diversity-combining techniques,” *IEEE Trans. Vehicular Technology*, vol. 48, pp. 1165–1181, Jul. 1999.
- [10] R. Zhang, Y.-C. Liang, C. C. Chai, and S. Cui, “Optimal beamforming for two-way multi-antenna relay channel with analogue network coding,” *IEEE J. Sel. Areas Commun.*, vol. 27, pp. 699–712, Jun. 2009.
- [11] P. Lioliou, M. Viberg, and M. Coldrey, “Performance analysis of relay channel estimation,” in *Proc. IEEE Asilomar Conference on Signals, Systems, and Computers*, Pacific Grove, CA, USA, Nov. 2009, pp. 1533–1537.
- [12] O. Muñoz-Medina, J. Vidal, and A. Agustín, “Linear transceiver design in nonregenerative relays with channel state information,” *IEEE Trans. Signal Process.*, vol. 55, pp. 2593–2604, Jun. 2007.
- [13] A. Høst-Madsen, “On the capacity of wireless relaying,” in *Proc. IEEE 56th Vehicular Technology Conference*, vol. 3, 2002, pp. 1333–1337.
- [14] R. Vaze and R. W. Heath, “On the capacity and diversity-multiplexing tradeoff of the two-way relay channel,” *IEEE Trans. Inf. Theory*, vol. 57, pp. 4219–4234, Jul. 2011.
- [15] N. Bornhorst, M. Pesavento, and A. B. Gershman, “Distributed beamforming for multi-group multicasting relay networks,” *IEEE Trans. Signal Process.*, vol. 60, pp. 221–232, Jan. 2012.
- [16] C. Schnurr, S. Stanczak, and T. Oechtering, “Coding theorems for the restricted half-duplex two-way relay channel with joint decoding,” in *Proc. IEEE International Symposium on Information Theory*, Toronto, Canada, July 2008.
- [17] J. N. Laneman and G. W. Wornell, “Distributed space-time coded protocols for exploiting cooperative diversity in wireless,” *IEEE Trans. Inf. Theory*, vol. 49, pp. 2415–2425, Oct. 2003.

- [18] J. N. Laneman, D. N. C. Tse, and G. W. Wornell, "Cooperative diversity in wireless networks: Efficient protocols and outage behavior," *IEEE Trans. Inf. Theory*, vol. 50, pp. 3062–3080, Dec. 2004.
- [19] B. Rankov and A. Wittneben, "Spectral efficient protocols for half-duplex fading relay channels," *IEEE J. Sel. Areas Commun.*, vol. 25, pp. 379–389, Feb. 2007.
- [20] K. Phan, T. Le-Ngoc, S. Vorobyov, and C. Tellambura, "Power allocation in wireless multi-user relay networks," *IEEE Trans. Wireless Commun.*, vol. 8, pp. 2535–2545, May 2009.
- [21] S. A. Jafar, K. S. Gomadam, and C. Huang, "Duality and rate optimization for multiple access and broadcast channels with amplify-and-forward relays," *IEEE Trans. Inf. Theory*, vol. 53, pp. 3350–3370, Oct. 2007.
- [22] C. T. K. Ng and G. J. Foschini, "Transmit signal and bandwidth optimization in multiple-antenna relay channels," *IEEE Trans. Commun.*, vol. 59, pp. 2987–2992, Nov. 2011.
- [23] B. Rankov and A. Wittneben, "On the capacity of relay-assisted wireless MIMO channels," in *Proc. 5th IEEE Workshop on Signal Processing Advances in Wireless Commun.*, Lisbon, Portugal, Jul. 2004, pp. 323–327.
- [24] H. Sampath, P. Stoica, and A. Paulraj, "Generalized linear precoder and decoder design for MIMO channels using the weighted MMSE criterion," *IEEE Trans. Commun.*, vol. 49, pp. 2198–2206, Dec. 2001.
- [25] S. Serbetli and A. Yener, "Transceiver optimization for multiuser MIMO systems," *IEEE Trans. Signal Process.*, vol. 52, pp. 214–226, Jan. 2004.
- [26] A. Zanella, M. Chiani, and M. Z. Win, "MMSE reception and successive interference cancellation for MIMO system with high spectral efficiency," *IEEE Trans. Wireless Commun.*, vol. 4, pp. 1244–1253, May 2005.
- [27] K. Sayana, S. Nagaraj, and S. B. Gelfand, "A MIMO zero forcing receiver with soft interference cancellation for BICM," *IEEE Workshop on Signal Process. Commun.*, vol. 4, pp. 837–839, 2005.

- [28] R. Zhang, C. C. Chai, and Y.-C. Liang, "Joint beamforming and power control for multiantenna relay broadcast channel with QoS constraints," *IEEE Trans. Signal Process.*, vol. 57, pp. 726–737, Feb. 2009.
- [29] S. Fazeli-Dehkordy, S. Shahbazpanahi, and S. Gazor, "Multiple peer-to-peer communications using a network of relays," *IEEE Trans. Signal Process.*, vol. 57, pp. 3053–3062, Aug. 2009.
- [30] C.-B. Chae, T. Tang, R. W. Heath, Jr., and S. Cho, "MIMO relaying with linear processing for multiuser transmission in fixed relay networks," *IEEE Trans. Signal Process.*, vol. 56, pp. 727–738, Feb. 2008.
- [31] B. K. Chalise and L. Vandendorpe, "Optimization of MIMO relays for multipoint-to-multipoint communications: Nonrobust and robust designs," *IEEE Trans. Signal Process.*, vol. 58, pp. 6355–6368, Dec. 2010.
- [32] M. Yuksel and E. Erkip, "Multiple-antenna cooperative wireless systems: A diversity-multiplexing tradeoff perspective," *IEEE Trans. Inf. Theory*, vol. 53, pp. 3371–3393, Oct. 2007.
- [33] Y. Rong and F. Gao, "Optimal beamforming for non-regenerative MIMO relays with direct link," *IEEE Commun. Lett.*, vol. 13, pp. 926–928, Dec. 2009.
- [34] Y. Rong, "Optimal joint source and relay beamforming for MIMO relays with direct link," *IEEE Commun. Lett.*, vol. 14, pp. 390–392, May 2010.
- [35] P. Frenger, "Turbo decoding for wireless systems with imperfect channel estimates," *IEEE Trans. Commun.*, vol. 48, pp. 1437–1440, Sep. 2000.
- [36] Y. Rong and M. R. A. Khandaker, "On uplink-downlink duality of multi-hop MIMO relay channel," *IEEE Trans. Wireless Commun.*, vol. 10, pp. 1923–1931, Jun. 2011.
- [37] T. Tang, C. B. Chae, R. W. Heath, Jr., and S. Cho, "On achievable sum rates of a multiuser MIMO relay channel," in *Proc. of IEEE ISIT*, Seattle, USA, Jul. 2006, pp.1026–1030.
- [38] Y. Rong and Y. Hua, "Optimality of diagonalization of multihop MIMO relays," *IEEE Trans. Wireless Commun.*, vol. 8, pp. 6068–6077, Dec. 2009.

- [39] Y. Rong, "Simplified algorithms for optimizing multiuser multi-hop MIMO relay systems," *IEEE Trans. Commun.*, vol. 59, pp. 2896–2904, Oct. 2011.
- [40] I. Hammerström and A. Wittneben, "Power allocation schemes for amplify-and-forward MIMO-OFDM relay links," *IEEE Trans. Wireless Commun.*, vol. 6, pp. 2798–2802, Aug. 2007.
- [41] K. S. Gomadam and S. A. Jafar, "Duality of MIMO multiple access channel and broadcast channel with amplify-and-forward relays," *IEEE Trans. Commun.*, vol. 58, pp. 211–217, Jan. 2010.
- [42] F. Gao, T. Cui, and A. Nallanathan, "On channel estimation and optimal training design for amplify and forward relay networks," *IEEE Trans. Wireless Commun.*, vol. 7, pp. 1907–1916, May 2008.
- [43] F. Gao, B. Jiang, X. Gao, and X.-D. Zhang, "Superimposed training based channel estimation for OFDM modulated amplify-and-forward relay networks," *IEEE Trans. Commun.*, vol. 59, pp. 2029–2039, Jul. 2011.
- [44] R. Mo, Y. H. Chew, and C. Yuen, "Information rate and relay precoder design for amplify-and-forward MIMO relay networks with imperfect channel state information," *IEEE Trans. Vehicular Technology*, vol. 61, pp. 3958–3968, Nov. 2012.
- [45] S. Jin, M. R. McKay, C. Zhong, and K.-K. Wong, "Ergodic capacity analysis of amplify-and-forward MIMO dual-hop systems," *IEEE Trans. Inf. Theory*, vol. 56, pp. 2204–2224, May 2010.
- [46] R. H. Y. Louie, Y. Li, H. A. Suraweera, and B. Vucetic, "Performance analysis of beamforming in two hop amplify and forward relay networks with antenna correlation," *IEEE Trans. Wireless Commun.*, vol. 8, pp. 3132–3141, Jun. 2009.
- [47] B. Wang, J. Zhang, and A. Høst-Madsen, "On the capacity of MIMO relay channels," *IEEE Trans. Inf. Theory*, vol. 51, pp. 29–43, Jan. 2005.
- [48] A. A. Nasir, S. Durrani, and R. A. Kennedy, "Blind timing and carrier synchronization in decode and forward cooperative systems," in *Proc. IEEE Int. Conf. Commun.*, Kyoto, Japan, Jun. 5-9, 2011.

- [49] E. Chiu, V. K. N. Lau, S. Zhang, and B. S. M. Mok, "Precoder design for multi-antenna partial decode-and-forward (PDF) cooperative systems with statistical CSIT and MMSE-SIC receivers," *IEEE Trans. Wireless Commun.*, vol. 11, pp. 1343–1349, Apr. 2012.
- [50] S. Karmakar and M. K. Varanasi, "The diversity-multiplexing tradeoff of the dynamic decode-and-forward protocol on a MIMO half-duplex relay channel," *IEEE Trans. Inf. Theory*, vol. 57, pp. 6569–6590, Oct. 2011.
- [51] S. Simoens, O. Muñoz-Medina, J. Vidal, and A. D. Coso, "Compress-and-forward cooperative MIMO relaying with full channel state information," in *Proc. IEEE Signal Theory and Commun.*, Nov. 2008.
- [52] J. Jiang, J. Thompson, H. Sun, and P. Grant, "Performance assessment of virtual multiple-input multiple-output systems with compress-and-forward cooperation," *IET Commun.*, vol. 6, pp. 1456–1465, 2011.
- [53] S. Karmakar and M. K. Varanasi, "Diversity-multiplexing tradeoff for the MIMO static half-duplex relay," *IEEE Trans. Inf. Theory*, vol. 58, pp. 3356–3368, Dec. 2012.
- [54] X. Tang and Y. Hua, "Optimal design of non-regenerative MIMO wireless relays," *IEEE Trans. Wireless Commun.*, vol. 6, pp. 1398–1407, Apr. 2007.
- [55] C. K. Lo, S. Vishwanath, and R. W. Heath, Jr., "Rate bounds for MIMO relay channels using precoding," in *Proc. IEEE GLOBECOM*, St. Louis, MO, USA, Dec. 2005, pp.1172–1176.
- [56] T. Kong and Y. Hua, "Optimal channel estimation and training design for MIMO relays," in *Proc. IEEE Asilomar Conference on Signals, Systems, and Computers*, Pacific Grove, CA, Nov. 2010, pp. 663–667.
- [57] W. Guan and H. Luo, "Joint MMSE transceiver design in non-regenerative MIMO relay systems," *IEEE Commun. Lett.*, vol. 12, pp. 517–519, Jul. 2008.
- [58] Y. Rong, "Linear non-regenerative multicarrier MIMO relay communications based on MMSE criterion," *IEEE Trans. Commun.*, vol. 58, pp. 1913–1923, Jul. 2010.

- [59] Z. Fang, Y. Hua, and J. C. Koshy, "Joint source and relay optimization for a non-regenerative MIMO relay," *IEEE Workshop on Sensor Array and Multichannel Process.*, pp. 239–243, Jul. 2006.
- [60] Y. Rong, X. Tang, and Y. Hua, "A unified framework for optimizing linear non-regenerative multicarrier MIMO relay communication systems," *IEEE Trans. Signal Process.*, vol. 57, pp. 4837–4851, Dec. 2009.
- [61] Y. Yu and Y. Hua, "Power allocation for a MIMO relay system with multiple-antenna users," *IEEE Trans. Signal Process.*, vol. 58, pp. 2823–2835, May 2010.
- [62] Y. Fan and J. Thompson, "MIMO configurations for relay channels: Theory and practice," *IEEE Trans. Wireless Commun.*, vol. 6, pp. 1774–1786, May 2007.
- [63] Y. Rong, "Non-regenerative multicarrier MIMO relay communications based on minimization of mean-squared error," in *Proc. IEEE ICC*, Dresden, Germany, Jun. 2009.
- [64] Y. Rong and M. R. A. Khandaker, "Channel estimation of dual-hop MIMO relay system via parallel factor analysis," in *Proc. 17th Asia-Pacific Conf. Commun.*, Sabah, Malaysia, Oct. 2–5, 2011.
- [65] Y. Rong, "Multi-hop non-regenerative MIMO relays-QoS considerations," *IEEE Trans. Signal Process.*, vol. 59, pp. 290–303, Jan. 2011.
- [66] C. Xing, S. Ma, Y. C. Wu, and T. S. Ng, "Transceiver design for dual-hop non-regenerative MIMO-OFDM relay systems under channel uncertainties," *IEEE Trans. Signal Process.*, vol. 58, pp. 6325–6339, Dec. 2010.
- [67] M. R. A. Khandaker and Y. Rong, "Joint source and relay optimization for multiuser MIMO relay communication systems," in *Proc. 4th Int. Conf. Signal Process. Commun. Systems*, Gold Coast, Australia, Dec. 13–15, 2010.
- [68] C. Song, K.-J. Lee, and I. Lee, "MMSE based transceiver designs in closed-loop non-regenerative MIMO relaying systems," *IEEE Trans. Wireless Commun.*, vol. 9, pp. 2310–2319, Jul. 2010.
- [69] G. Li, Y. Wang, T. Wu, and J. Huang, "Joint linear filter design in multi-user non-regenerative MIMO-relay systems," in *Proc. IEEE Int. Conf. Commun.*, Dresden, Germany, pp. 1–6, Jun. 2009.

- [70] S. Jang, J. Yang, and D. K. Kim, "Minimum MSE design for multiuser MIMO relay," *IEEE Commun. Lett.*, vol. 14, pp. 812–814, Sep. 2010.
- [71] Y. Rong, "Robust design for linear non-regenerative MIMO relays with imperfect channel state information," *IEEE Trans. Signal Process.*, vol. 59, pp. 2455–2460, May 2011.
- [72] K.-J. Lee, H. Sung, E. Park, and I. Lee, "Joint optimization for one and two-way MIMO AF multiple-relay systems," *IEEE Trans. Wireless Commun.*, vol. 9, pp. 3671–3681, Dec. 2010.
- [73] A. S. Behbahani, R. Merched, and A. M. Eltawil, "Optimizations of a MIMO relay network," *IEEE Trans. Signal Process.*, vol. 56, pp. 5062–5073, Oct. 2008.
- [74] A. Toding, M. R. A. Khandaker, and Y. Rong, "Optimal joint source and relay beamforming for parallel MIMO relay networks," in *Proc. 6th Int. Conf. Wireless Commun., Networking and Mobile Computing*, Chengdu, China, Sep. 23–25, 2010.
- [75] Y. Rong, "Joint source and relay optimization for two-way linear non-regenerative MIMO relay communications," *IEEE Trans. Signal Process.*, vol. 60, pp. 6533–6546, Dec. 2012.
- [76] J. R. Barry, E. A. Lee, and D. G. Messerschmitt, "Capacity penalty due to ideal zero-forcing decision-feedback equalization," *IEEE Trans. Inf. Theory*, vol. 42, pp. 1062–1071, Jul. 1996.
- [77] F. Wang, S. C. Liew, and D. Guo, "Wireless MIMO switching with zero forcing and network coding," *IEEE J. Sel. Areas Commun.*, vol. 30, pp. 1452–1463, Sep. 2012.
- [78] J. Park, G. Lee, Y. Sung, and M. Yukawa, "Coordinated beamforming with relaxed zero forcing: The sequential orthogonal projection combining method and rate control," *IEEE Trans. Signal Process.*, vol. 61, pp. 3100–3112, Jun. 2013.
- [79] C. Hellings, S. Herrmann, and W. Utschick, "Carrier cooperation can reduce the transmit power in parallel MIMO broadcast channels with zero-forcing," *IEEE Trans. Signal Process.*, vol. 61, pp. 3021–3027, Jun. 2013.
- [80] H. Kim, H. Yu, Y. Sung, and Y. H. Lee, "An efficient algorithm for zero-forcing coordinated beamforming," *IEEE Commun. Lett.*, vol. 16, pp. 994–997, Jul. 2012.

- [81] W. Li and M. Latva-aho, "An efficient channel block diagonalization method for generalized zero-forcing assisted MIMO broadcasting systems," *IEEE Trans. Wireless Commun.*, vol. 10, pp. 739–744, Mar. 2011.
- [82] A. H. Mehana and A. Nosratinia, "Diversity of MMSE MIMO receivers," *IEEE Trans. Info. Theory*, vol. 58, pp. 6788–6805, Nov. 2012.
- [83] J. Wang, O. Y. Wen, and S. Li, "Soft-output MMSE MIMO detector under ML channel estimation and channel correlation," *IEEE Trans. Signal Process.*, vol. 16, pp. 667–670, Aug. 2009.
- [84] P. Li, D. Paul, R. Narasimhan, and J. Cioffi, "On the distribution of SINR for the MMSE MIMO receiver and performance analysis," *IEEE Trans. Inf. Theory*, vol. 52, pp. 271–286, Jan. 2006.
- [85] K. Kansanen and T. Matsumoto, "An analytical method for MMSE MIMO turbo equalizer EXIT chart computation," *IEEE Trans. Wireless Commun.*, vol. 6, pp. 59–63, Jan. 2007.
- [86] J. Wang and M. Bengtsson, "Joint optimization of the worst-case robust MMSE MIMO transceiver," *IEEE Trans. Signal Process.*, vol. 18, pp. 295–298, May 2011.
- [87] L. Weng and R. D. Murch, "Multi-user MIMO relay system with self-interference cancellation," in *Proc. IEEE WCNC*, Kowloon, China, Mar. 2007, pp. 958–962.
- [88] T. Taniguchi, N. B. Ramli, and Y. Karasawa, "Design of multiuser MIMO AF relay system with interference cancellation," in *Proc. 6th Int. Wireless Commun. Mobile Comput. Conf.*, Caen, France, Jun. 2010, pp. 1075–1080.
- [89] Y. Rong, "Optimal linear non-regenerative multi-hop MIMO relays with MMSE-DFE receiver at the destination," *IEEE Trans. Wireless Commun.*, vol. 9, pp. 2268–2279, Jul. 2010.
- [90] A. Toding, M. R. A. Khandaker, and Y. Rong, "Joint source and relay optimization for parallel MIMO relays using MMSE-DFE receiver," in *Proc. 16th Asia-Pacific Conf. Commun.*, Auckland, New Zealand, pp. 12–16, Nov. 1-3, 2010.
- [91] L. Vandendorpe, J. Louveaux, B. Maison, and A. Chevreuil, "About the asymptotic performance of MMSE MIMO DFE for filter-bank based multicarrier transmission," *IEEE Trans. Commun.*, vol. 47, pp. 1472–1475, Oct. 1999.

-
- [92] Y. Zhang, H. Luo, and W. Chen, "Efficient relay beamforming design with SIC detection for dual-hop MIMO relay networks," *IEEE Trans. Vehicular Technology*, vol. 59, pp. 4192–4197, Oct. 2010.
- [93] J. Choi and H. Nguyen, "SIC-based detection with list and lattice reduction for MIMO channels," *IEEE Trans. Vehicular Technology*, vol. 58, pp. 3786–3790, Sep. 2009.
- [94] C. Ling, W. H. Mow, and L. Gan, "Dual-lattice ordering and partial lattice reduction for SIC-based MIMO detection," *IEEE J. Sel. Signal Process.*, vol. 3, pp. 975–985, Dec. 2009.
- [95] H. Kwon, J. Lee, and I. Kang, "Successive interference cancellation via rank-reduced maximum a posteriori detection," *IEEE Trans. Commun.*, vol. 61, pp. 628–637, Feb. 2013.
- [96] Y.-C. Liang, E. Y. Cheu, L. Bai, and G. Pan, "On the relationship between MMSE-SIC and BI-GDFE receivers for large multiple-input multiple-output channels," *IEEE Trans. Signal Process.*, vol. 56, pp. 3627–3637, Aug. 2008.
- [97] H. Zhang, H. Dai, and B. L. Hughes, "Analysis on the diversity-multiplexing tradeoff for ordered MIMO SIC receivers," *IEEE Trans. Commun.*, vol. 57, pp. 125–133, Jan. 2009.
- [98] T.-H. Liu, J.-Y. Jiang, and Y.-S. Chu, "A low-cost MMSE-SIC detector for the MIMO system: Algorithm and hardware implementation," *IEEE Trans. Circuits Sys.*, vol. 58, pp. 56–61, Jan. 2011.
- [99] X. Dai, "Enhancing the performance of the SIC-MMSE iterative receiver for coded MIMO systems via companding," *IEEE Commun. Lett.*, vol. 16, pp. 921–924, Jun. 2012.
- [100] P. Liu and I.-M. Kim, "Exact and closed-form error performance analysis for hard MMSE-SIC detection in MIMO systems," *IEEE Trans. Commun.*, vol. 59, pp. 2463–2477, Sep. 2011.
- [101] T.-H. Liu, "Some results for the fast MMSE-SIC detection in spatially multiplexed MIMO systems," *IEEE Trans. Wireless Commun.*, vol. 8, pp. 5443–5448, Nov. 2009.

- [102] J. Ham, K. Kim, S. Kim, and C. Lee, "Link-adaptive MIMO systems with ordered SIC receiver using stream-ordering algorithms in multiuser environments," *IEEE Trans. Vehicular Technology*, vol. 57, pp. 3224–3230, Sep. 2008.
- [103] T.-H. Liu and Y.-L. Y. Liu, "Modified fast recursive algorithm for efficient MMSE-SIC detection of the V-BLAST system," *IEEE Trans. Wireless Commun.*, vol. 7, pp. 3713–3717, Oct. 2008.
- [104] C.-W. Huang, P.-A. Ting, and C.-C. Huang, "A novel message passing based MIMO-OFDM data detector with a progressive parallel ICI canceller," *IEEE Trans. Wireless Commun.*, vol. 10, pp. 1260–1268, Apr. 2011.
- [105] M. Grant and S. Boyd, "Cvx: Matlab software for disciplined convex programming (web page and software)." <http://cvxr.com/cvx>, Apr. 2010.
- [106] S. Boyd and L. Vandenberghe, *Convex Optimization*. Cambridge, U. K.: Cambridge University Press, 2004.
- [107] D. P. Bertsekas, *Nonlinear Program*. 2nd Edition, Athena Scientific, 1999.
- [108] K. B. P. and M. S. Petersen, *The Matrix Cookbook*. [Online]. Available: <http://matrixcookbook.com>.
- [109] A. W. Marshall and I. Olkin, *Inequalities: Theory of Majorization and Its Applications*. Academic Press, 1979.
- [110] Y. Jiang, W. W. Hager, and J. Li, "The generalized triangular decomposition," *Mathematics of Computation*, vol. 77, pp. 1037–1056, Apr. 2008.

Every reasonable effort has been made to acknowledge the owners of copyright material. I would be pleased to hear from any copyright owner who has been omitted or incorrectly acknowledged.